

Radiation from leptons in crystals, theory

Victor Tikhomirov

Institute for Nuclear Problems Minsk, Belarus

Outline

- *Circularly polarized* coherent bremmstrahlung and pair production
- Radiation in the MVROC conditions
- Radiation in the cut presence
- Conclusions

Unfortunately, most of the
Strong Field QED effects
need the LHC energy
for their observation

However
Circularly Polarized
Coherent Bremsstrahlung
and Pair Production
are observable at
GeV-TeV energies

Coherent bremsstrahlung

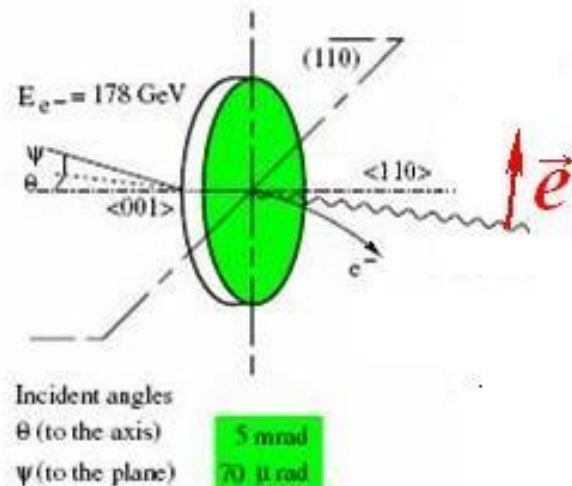
Predicted: Ferretti, Ter-Mikaelian, Dyson and Überall,..

Observed: first - Diambrini-Palazzi et al. (1960) in Frascati

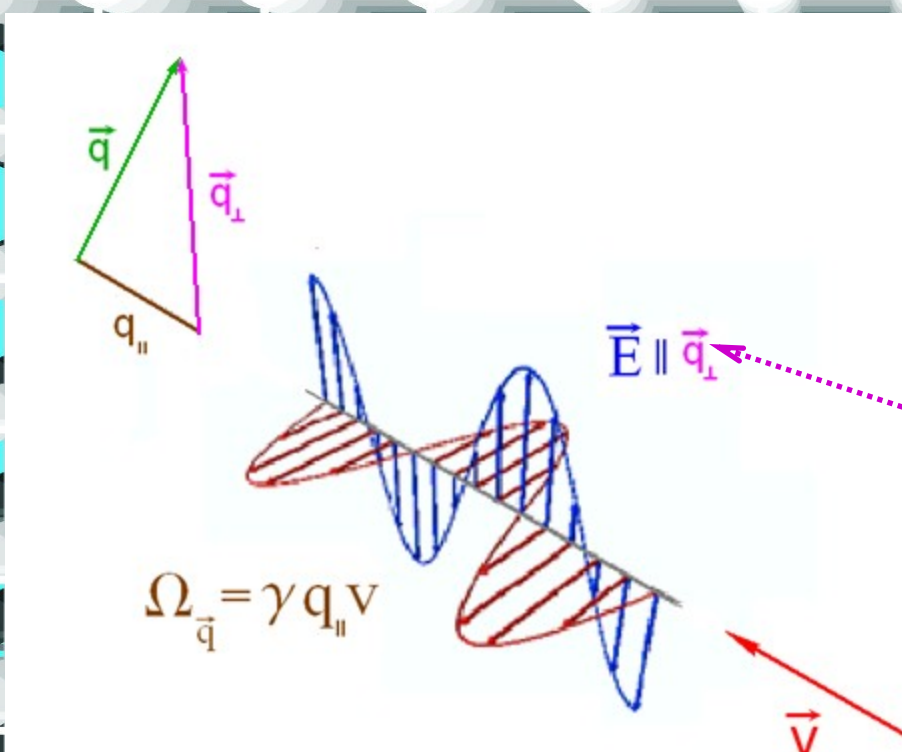
at present - Arends et al., Mainz (MAMI, 855 MeV),
Klein et al., Bonn (ELSA, 3 GeV),
Avakian et al., CERN (20-170 GeV),
Klein et al., Jeff. Lab. (6 GeV).

Polarization: linear

Jeff. Lab. $P_\gamma = 84\%$
for the production
of ρ and ω mesons



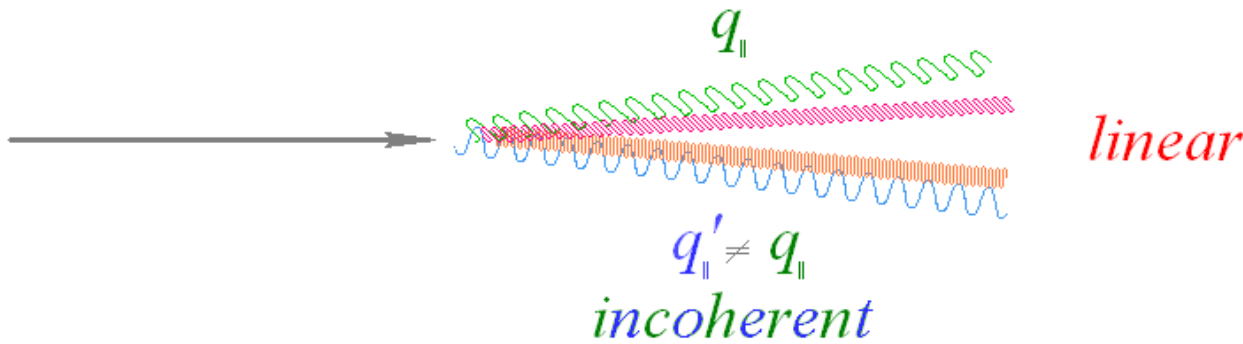
Crystal field can be represented by pseudophotons
with frequency $\Omega_{\vec{q}} = \gamma q_{||} v$
and linear polarization $\vec{E} \parallel \vec{q}_{\perp}$



$$V(\vec{r}) = \sum_{\vec{q}} V_{\vec{q}} e^{i\vec{q}\vec{r}}$$

$$\vec{E}(\vec{r}) = -\vec{\nabla} V(\vec{r}) = -i \sum_{\vec{q}} \vec{q} V_{\vec{q}} e^{i\vec{q}\vec{r}}$$

CB is (has been!) linearly polarized



Coherent Bremsstrahlung \sim backward Compton scattering
of linearly polarized photons with energies

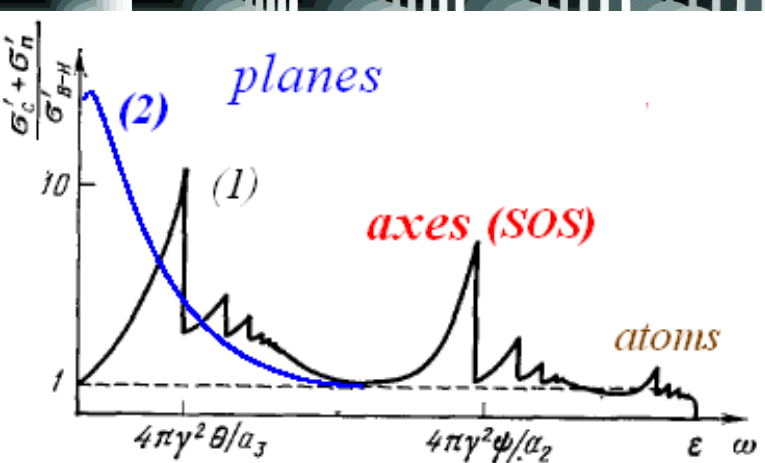
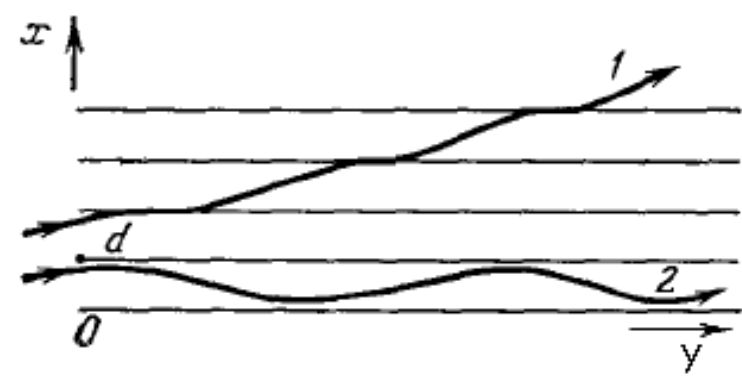
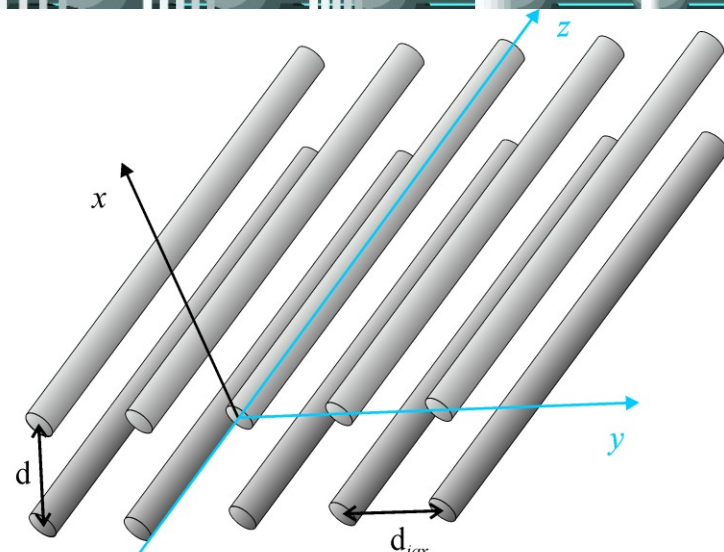
$$\Omega_{\vec{q}} = \gamma q_{\parallel} v$$

$\Omega_{\vec{q}} \sim \gamma_{\vec{q}}$ scattering is *incoherent*

\Rightarrow polarization remains *linear*

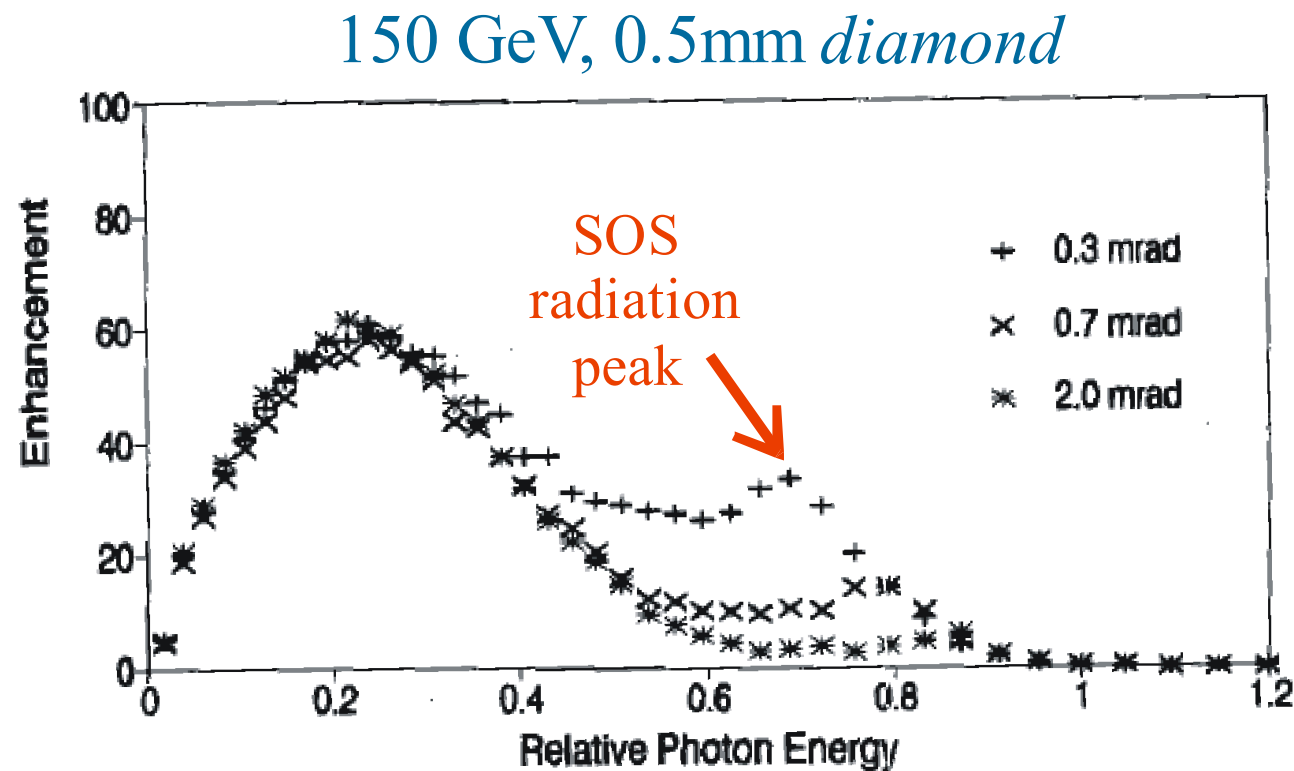
String-of-strings geometry (Lindhard; Akhiezer&Shul'ga)

motion in transverse plane



Experimental observation of hard radiation peak in string-of-strings geometry

R. Medenwaldt et al. PLB 281(1992)153



Coherent bremsstrahlung, coherent pair production, birefringence, and polarimetry
in the 20–170 GeV energy range using aligned crystals

A. Apyan,^{1,*} R. O. Avakian,¹ B. Badelek,² S. Ballestrero,^{3,4} C. Biino,^{4,5} I. Birol,⁶ P. Cenci,⁷ S. H. Connell,⁸ S. Eichblatt,⁶ T. Fonseca,⁶ A. Freund,⁹ B. Gorini,⁵ R. Groess,¹⁰ K. Ispirian,¹ T.J. Ketel,¹¹ Yu. V. Kononets,¹² A. Lopez,¹³ A. Mangiarotti,¹⁴ B. van Rens,¹¹ J.P.F. Sellschop,^{10,7} M. Shieh,⁶ P. Sona,¹⁴ V. Strakhovenko,¹⁵ E. Uggerhøj,^{16,8} U.I. Uggerhøj,¹⁷ G. Unel,¹⁸ M. Velasco,^{5,8} Z. Z. Vilakazi,^{10,11} and O. Wessely²

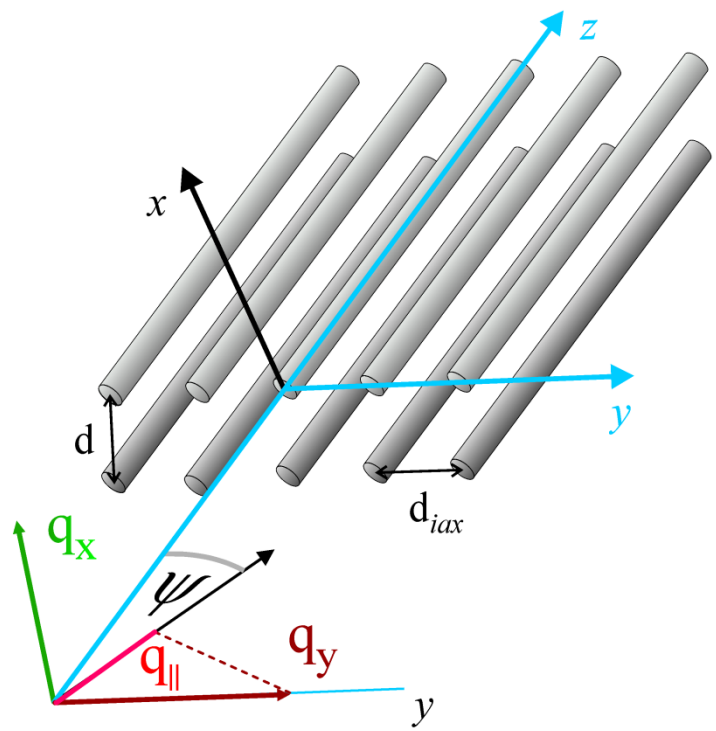
(NA59 Collaboration)

...using crystals, *only linear polarization* may be produced.

... Our measurements and our calculations indicate *low photon polarization* for the high-energy SOS photons.

Nevertheless, We'll show that **circular polarization** of radiation of positrons channeled in *bent crystals* with string-of-strings orientation **can be high!**

SOS radiation can be circularly polarized!



$$q_{1x} = \frac{2\pi}{d}, \quad q_{1y} = \frac{2\pi}{d_{inax}},$$
$$q_x = q_{1x}n_x, \quad q_y = q_{1y}n_y,$$
$$\vec{q} = q_x \vec{e}_x + q_y \vec{e}_y,$$
$$q_{||} = \vec{q}\vec{v}/v = \psi q_y \Rightarrow$$

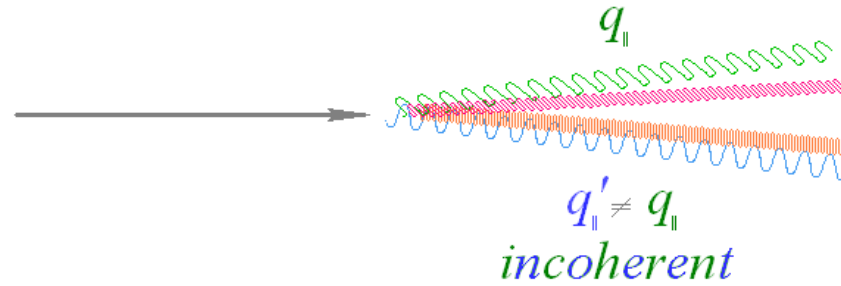
if $q_x = q_{1x}n_x \neq q'_x = q_{1x}n_x$

$$q_{||} = q'_{||}$$

different q_x , same $q_{||}$!

Coherence of “crystal photons” at SOS geometry allows to obtain **circular polarization**

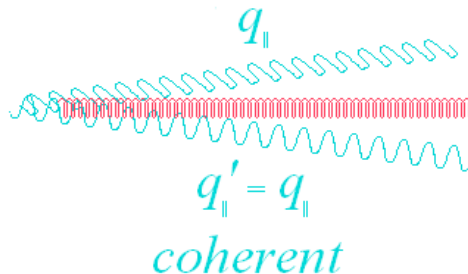
Coherent Bremsstrahlung



linear

$q'_{\parallel} \neq q_{\parallel}$
incoherent

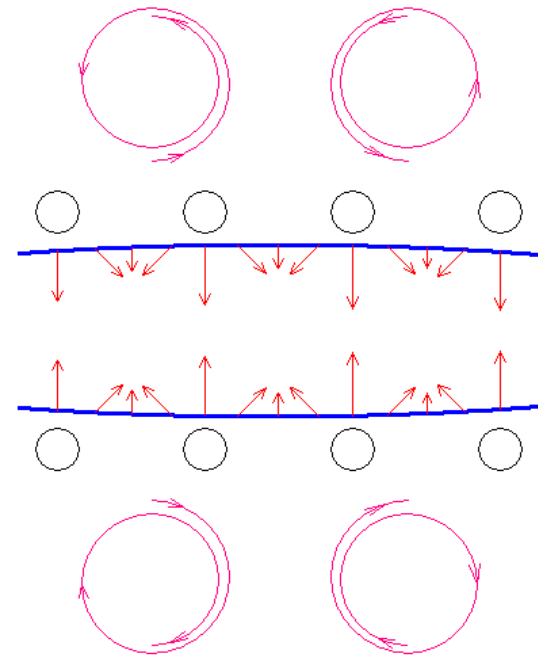
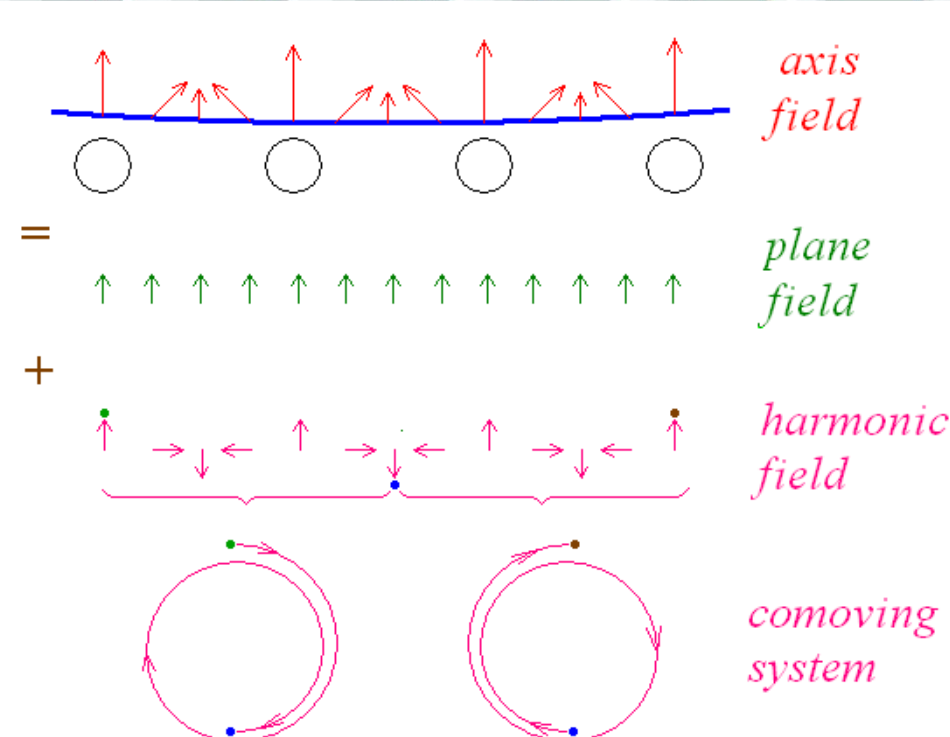
SOS radiation



elliptical

$q'_{\parallel} = q_{\parallel}$
coherent

Intuitive prove of crystal field harmonic circular polarization



CP is opposite on opposite channel sides!

“Mathematical prove” of crystal field harmonic circular polarization

V.V.Tikhomirov , JETP 109(1996)1188

Fourier decomposition of the axial potential

$$V(x, y) = \sum_{q_x, q_y} V(q_x, q_y) e^{iq_x x} e^{iq_y y},$$

where $q_x = 2\pi n_x/d$, $q_y = 2\pi n_y/d_{max}$, $n_{x,y} = 0, \pm 1, \pm 2, \dots$
 d is the inter-planar distance,
 d_{max} is the inter-axis distances inside the plane.

Planar potential

$$V(x) = \sum_{n_x=0, \pm 1, \pm 2, \dots} V(q_x) e^{iq_x x}.$$

Slowly varying amplitudes

$$E_{xn}(x) = 2 \sum_{n_x=0, \pm 1, \dots} V(q_x, q_y) q_x \sin(q_x x),$$

$$E_{yn}(x) = 2q_y \sum_{n_x=0, \pm 1, \dots} V(q_x, q_y) \cos(q_x x)$$

of the averaged crystal electric field

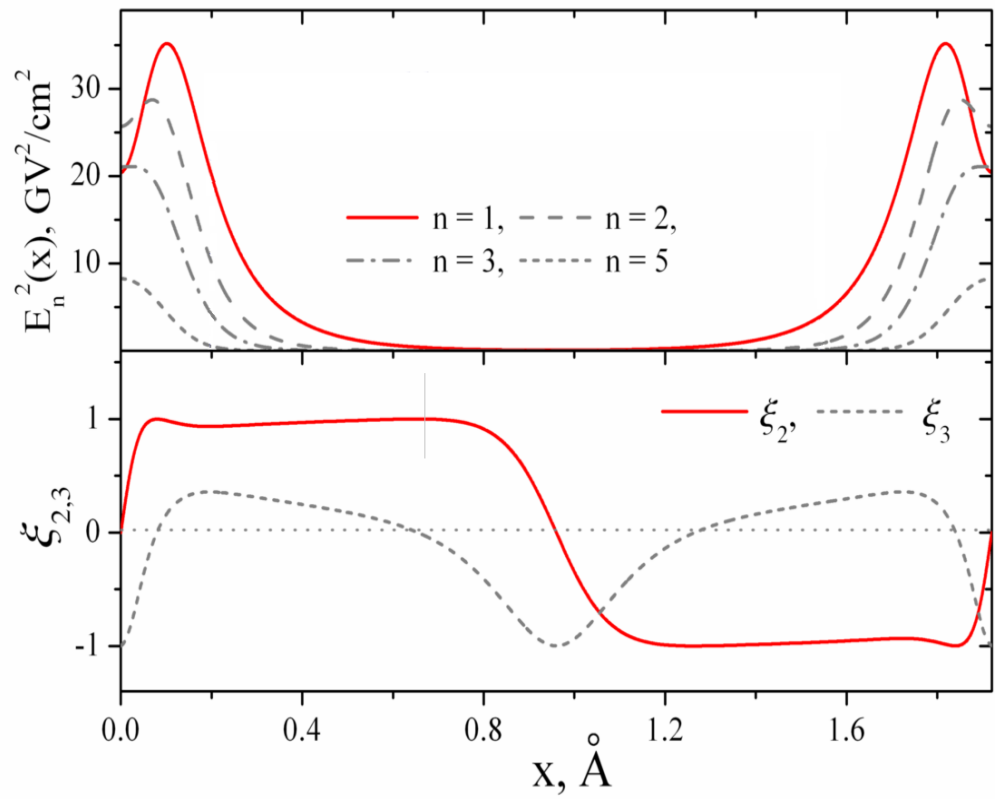
$$\mathbf{E} = -\vec{\nabla} V(x, y) = -\mathbf{n}_x V'(x) + \sum_{n=\pm 1, \pm 2, \dots} [\mathbf{n}_x E_{xn}(x) - i\mathbf{n}_y E_{yn}(x)] e^{iq_y y}.$$

Stokes parameters of the crystal field harmonic

$$\xi_{2n} = \frac{2E_{xn}E_{yn}}{E_n^2}, \quad \xi_{3n} = \frac{E_{xn}^2 - E_{yn}^2}{E_n^2}, \quad E_n = \sqrt{E_{xn}^2 + E_{yn}^2}.$$

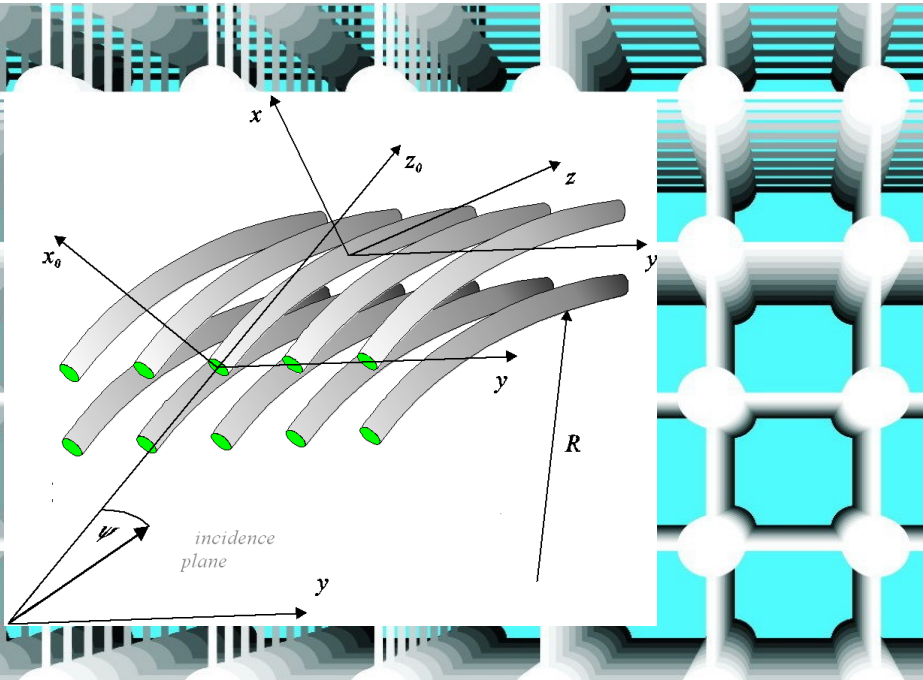
Space symmetry properties of the amplitudes

$$E_{xn}(d-x) = -E_{xn}(x), \quad E_{yn}(d-x) = E_{yn}(x)$$

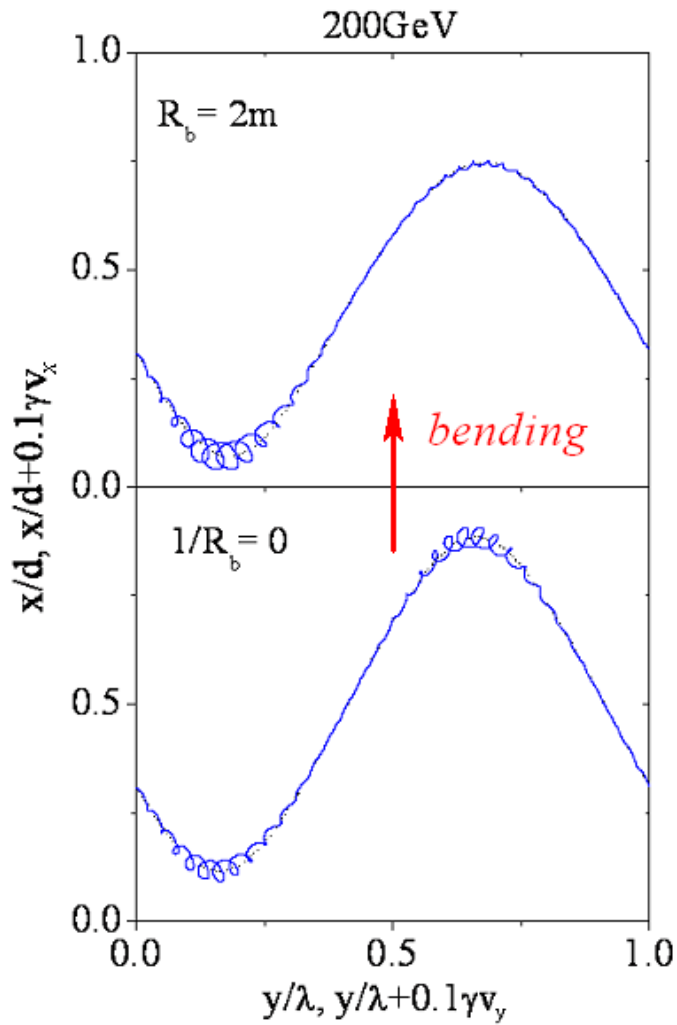


CP is opposite on opposite channel sides!

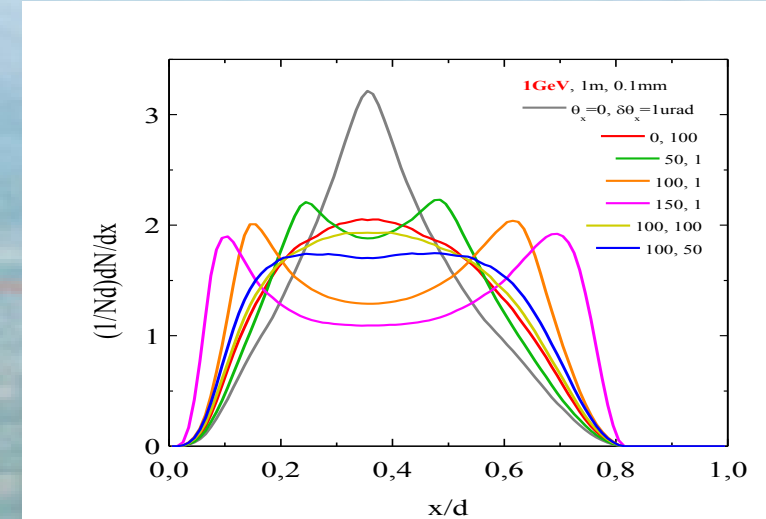
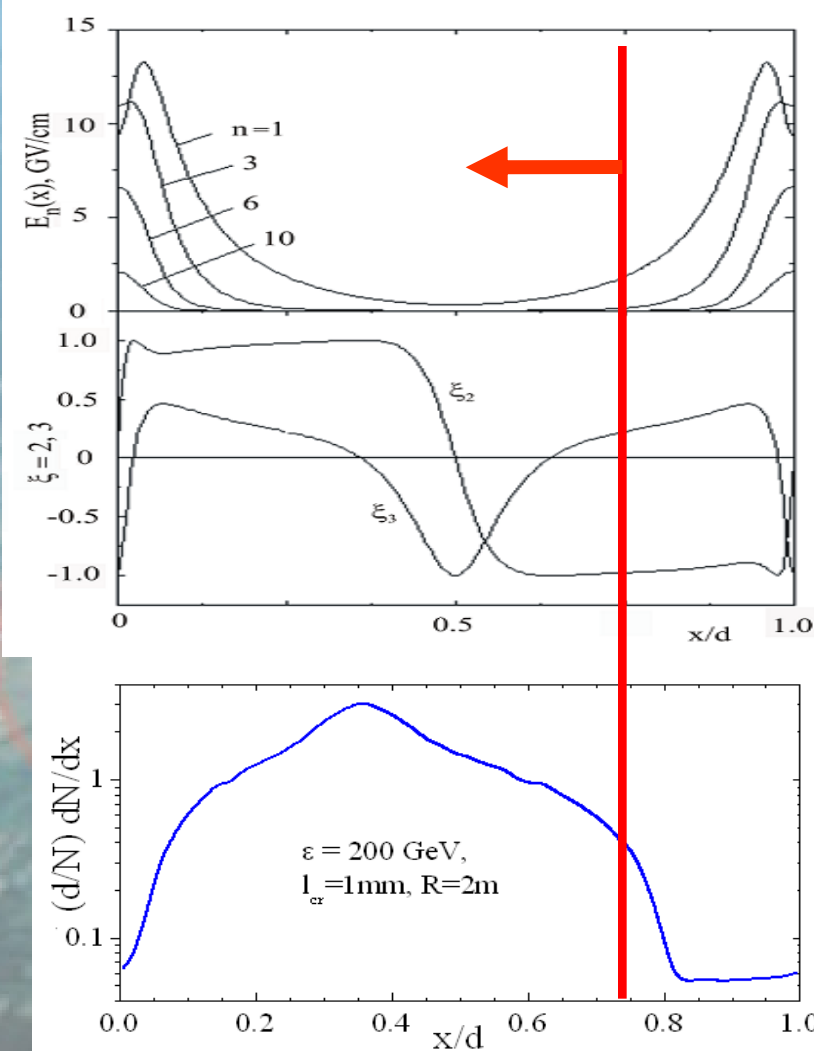
Crystal bending gives rise to a preferred spirality of positron trajectories



Projections on xy plane of positron trajectories (dots) and velocities (solid spirals) in Si crystal with (top) and without bending (bottom). Velocity components, measured in units of $0.1/\gamma$ are plotted from the corresponding positron coordinates. Velocity projections rotate in opposite directions near the opposite crystal planes (at $x \sim 0.15d$ and $x \sim 0.85d$). Crystal bending violates trajectory symmetry amplifying velocity oscillations at $x \sim 0.1d$ and diminishing them at $x \sim 0.7d$.



Channeled positrons move in the regions of specific circular polarization in bent crystals



It is really possible:

1. to depopulate
the region of $0.8 < x/d < 1$
2. to populate
the region of $x/d \sim 0.1$

A simplest “local coherent bremsstrahlung” theory allowing to evaluate circular polarization of emitted gamma quanta

Gamma-quantum polarization matrix

[V.M. Strakhovenko, Phys. Rev. A68:042901, 2003]:

$$\frac{d\omega_{ij}}{d\omega d^2\theta} = \frac{\alpha\omega^2}{16\pi^2\epsilon'} \int \int dt_1 dt_2 L_{ij} \exp \left\{ i\omega \frac{\epsilon}{\epsilon'} [t_1 - t_2 - \mathbf{n}(\mathbf{r}_1 - \mathbf{r}_2)] \right\}$$

$$L_{ij} = \varphi(\epsilon) [(\mathbf{e}_i \mathbf{v}_1)(\mathbf{e}_j \mathbf{v}_2) - (\mathbf{e}_j \mathbf{v}_2)(\mathbf{e}_i \mathbf{v}_1)] + 2[(\mathbf{e}_i \mathbf{v}_1)(\mathbf{e}_j \mathbf{v}_2) + (\mathbf{e}_j \mathbf{v}_2)(\mathbf{e}_i \mathbf{v}_1)] + \delta_{ij}(\mathbf{v}_1 \mathbf{v}_2 - 1 + \gamma^{-2}),$$

$$c = \hbar = 1, \quad \alpha = 1/137, \quad i, j = x, y$$

$$\epsilon' = \epsilon - \omega, \varphi = \epsilon/\epsilon' + \epsilon'/\epsilon,$$

$$\mathbf{v}_{1,2} = \mathbf{v}(t_{1,2}), \quad \mathbf{r}_{1,2} = \mathbf{r}(t_{1,2}).$$

Its expansion up to $O((\gamma\tau)^2)$ terms

$$d\omega_{ij} = \frac{i\alpha d\omega}{4\pi\gamma^2} \int_{-\infty}^{\infty} dt \int_{-\infty}^{\infty} \frac{d\tau}{\tau - i0} \times \left\{ \delta_{ij} \left[\frac{1}{4}(\varphi - 2)(\mathbf{g}_2 - \mathbf{g}_1)^2 + \frac{1}{\tau} \int_{-\tau/2}^{\tau/2} d\tau' \mathbf{g}^2(t + \tau') \right] + \frac{\varphi}{2} (g_{2i}g_{1j} - g_{2j}g_{1i}) - (g_{2i}g_{1j} + g_{2j}g_{1i}) \right\} \exp \left(-i \frac{\omega m^2}{2\epsilon\epsilon'} \right),$$

$$\mathbf{g}_{1,2} = \gamma \left[\mathbf{v}_\perp(t_{1,2}) - \frac{1}{\tau} \int_{-\tau/2}^{\tau/2} d\tau' \mathbf{v}_\perp(t + \tau') \right]$$

$$= -i \sum_{n=\pm 1, \pm 2, \dots} \frac{1}{mq_\parallel} [\mathbf{n}_x E_{xn}(x) - i\mathbf{n}_y E_{yn}(x)]$$

$$\times [\exp(\mp iq_\parallel\tau) - \sin(q_\parallel\tau/2)/(q_\parallel\tau/2)] \exp(iq_\parallel t + iq_y y_0), \quad q_\parallel = q_y \psi.$$

The “index” symmetry properties

$$E_{x-n}(x) = E_{xn}(x), \quad E_{y-n}(x) = -E_{yn}(x)$$

allow to obtain

$$d\omega_{ij} = \frac{i\alpha d\omega}{4\pi\gamma^2} \int_{-\infty}^{\infty} dt \int_{-\infty}^{\infty} \frac{d\tau}{\tau - i0} \sum_{n=\pm 1, \pm 3, \dots} \frac{1}{mq_\parallel^3} \times \left\{ \delta_{ij} E_n^3 [1 - f^2(\zeta) + (\varphi(\epsilon) - 2)\sin^2\zeta] - \varphi(\epsilon) E_{in} E_{jn} \epsilon_{ij} [\sin 2\zeta - 2f(\zeta) \sin\zeta] - 2E_{in} E_{jn} \delta_{ij} [\cos\zeta + f^2(\zeta) - 2f(\zeta) \cos\zeta] \right\} \exp \left(-i \frac{\omega m^2}{2\epsilon\epsilon'} \right),$$

$$\zeta = q_\parallel\tau/2, \quad f(\zeta) = \sin\zeta/\zeta.$$

Integration over τ leads to the “local” probability of gamma quantum emission having the “Compton scattering form”:

$$d\omega_{ij} = (A + B\partial^i)_{ij}/2,$$

$$(A, B) = \frac{\alpha}{\gamma^2} \sum_{n=1,3,\dots} \left(\frac{E_n}{mq_\parallel} \right)^3 (\mathbf{a}, \mathbf{b}) \theta(1 - \nu),$$

$$\mathbf{a} = \frac{\varphi(\epsilon)}{2} + 2\nu(1 - \nu), \quad \nu = \frac{\omega m^2}{2\epsilon\epsilon' |q_\parallel|},$$

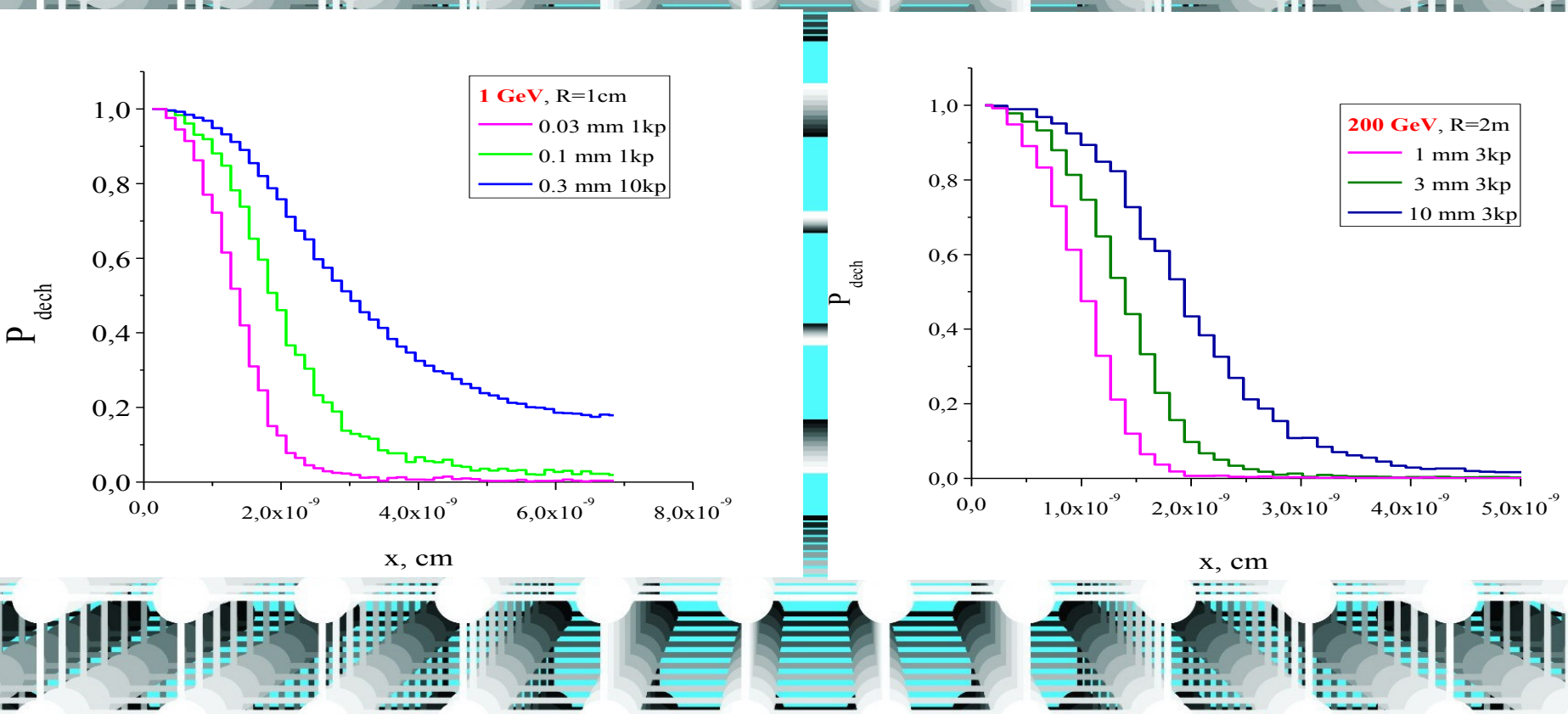
$$b_1 = 0, \quad b_3 = \xi_{3n} \varphi(\nu - 1/2), \quad b_3 = \xi_{3n} \nu^3,$$

$b_3 \propto \xi_{3n}$ TERM DESCRIBES GAMMA CIRCULAR POLARIZATION!

Strakhovenko:

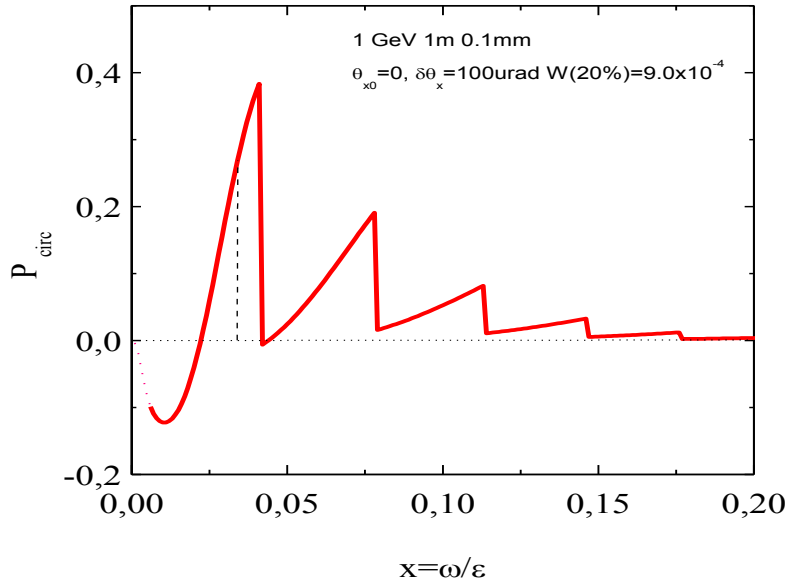
$$b_1 = \xi_{1n} \nu^3, \quad b_2 = 0, \quad b_3 = \xi_{3n} \nu^3.$$

Positron dechanneling probability vs initial transverse coordinate at $\theta = 0$



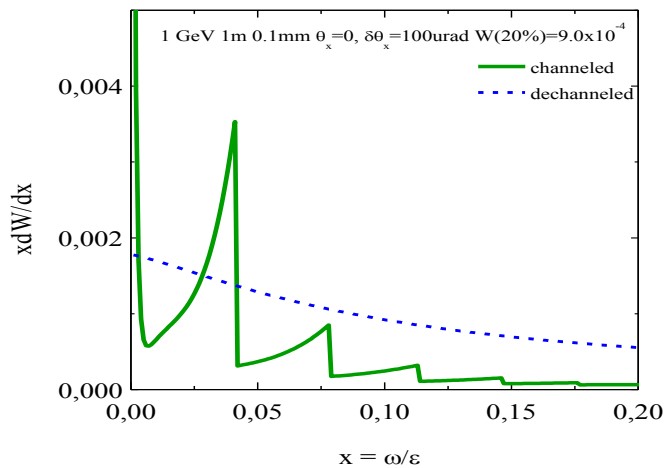
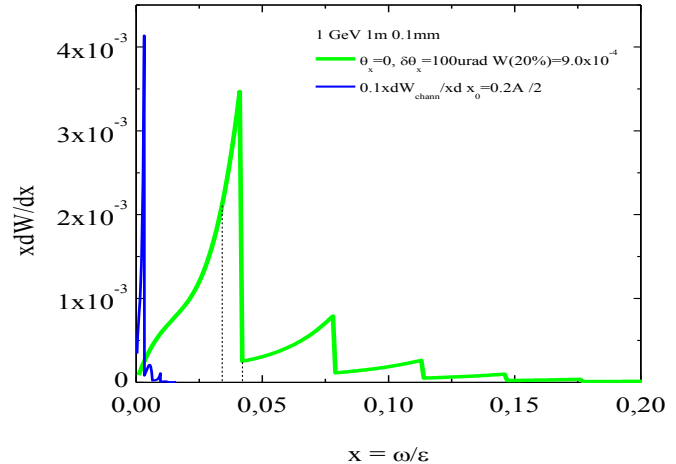
Positrons spend considerable time at $x \sim 0.2\text{\AA}$

Polarization and spectrum of 1 GeV channeled e^+

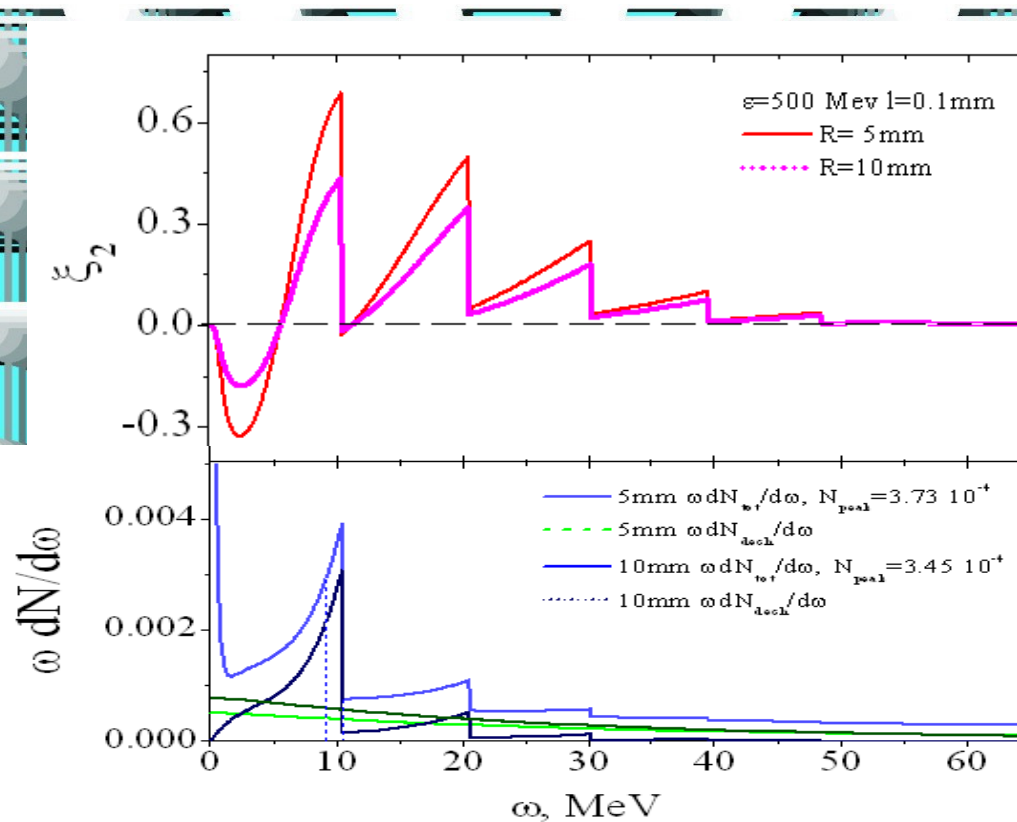


$$l_{cr} = 0.1\text{mm}, R = 1\text{cm}! \quad W \sim 10^{-3}$$

Compton scattering in magnetized iron can be used to measure gamma polarization!

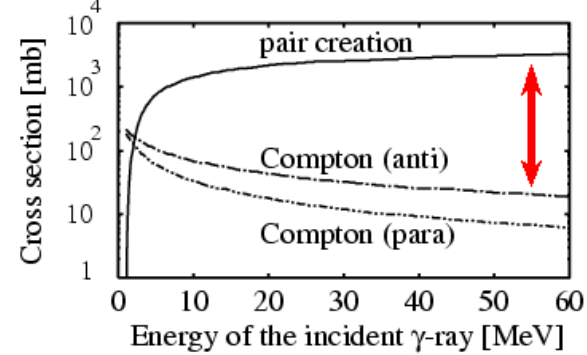


Polarization and spectrum of 500MeV channeled e⁺

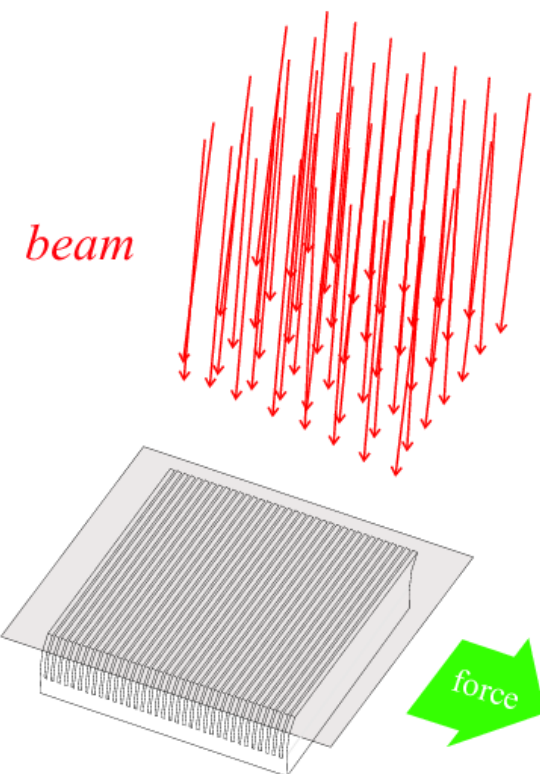


$I_{cr} = 0.1\text{mm}$, $R = 1\text{cm}!$ $W \sim 10^{-3}$

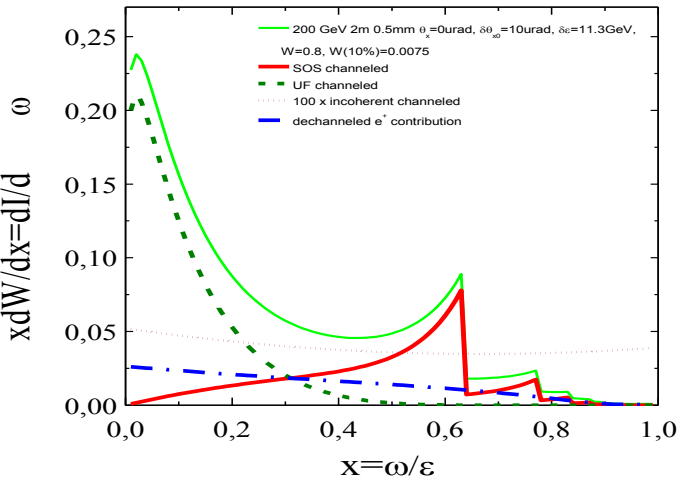
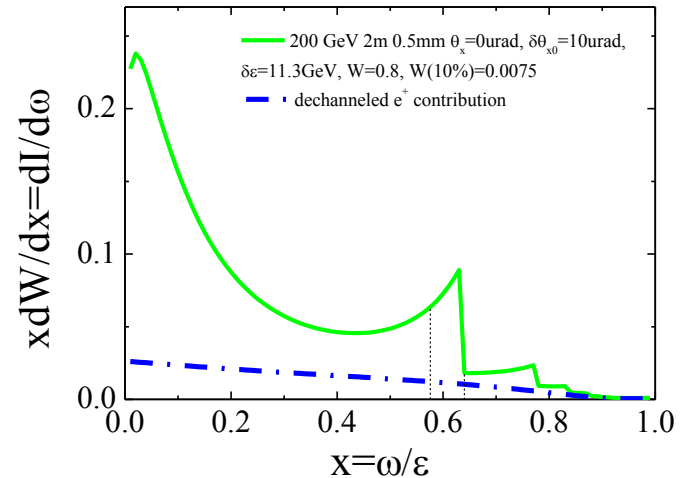
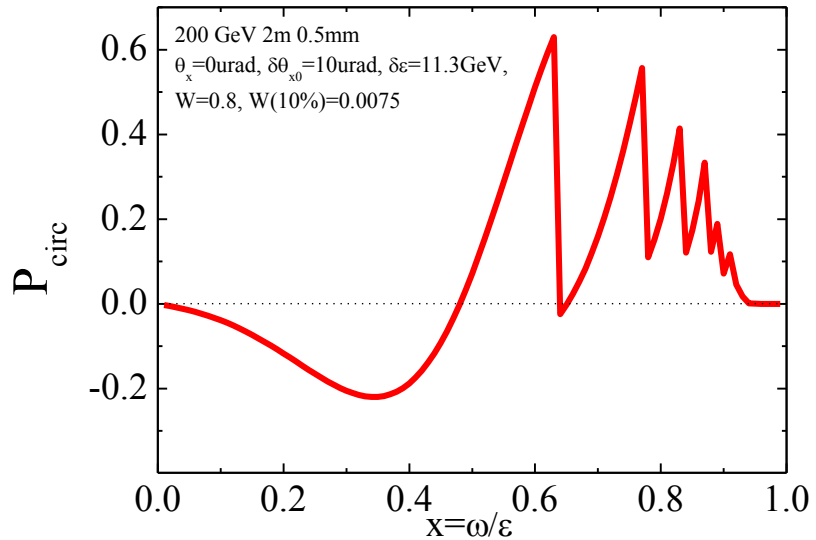
Compton scattering in magnetized iron can be used to measure gamma polarization!



A crystal assembly allowing to pass a **wide** particle beam through very **short** crystals bent with very **small** radius



Polarization and spectrum of 200 GeV channeled e⁺



$l_{cr} = 0.2\text{mm}$, $R = 2\text{m}$
– easily available!

$W \sim 10^{-2}$!

A new method to calculate the characteristics of radiation and pair production under high energies and arbitrary angles of particle incidence relative to the crystal planes

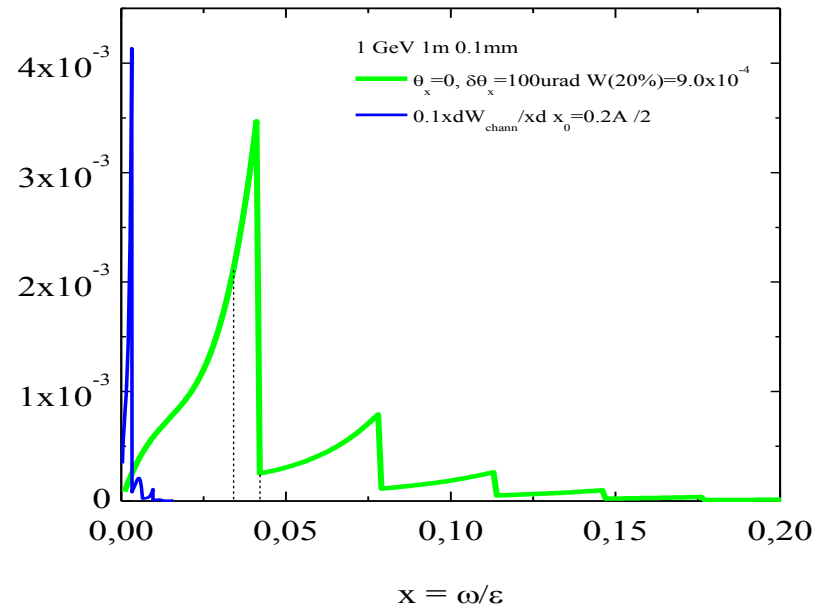
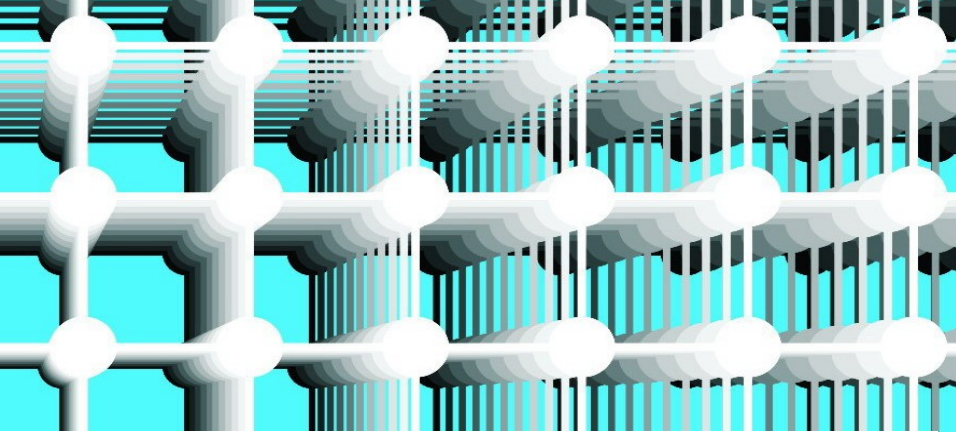
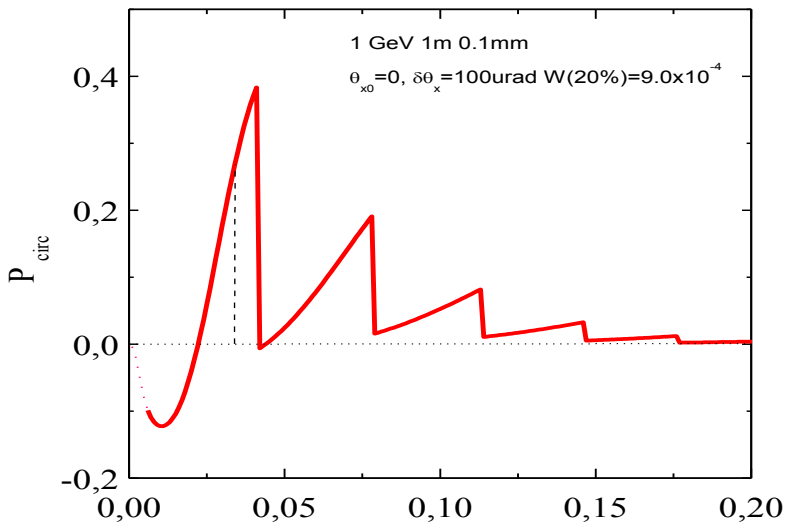
V.V. Tikhomirov

Institute of Nuclear Problems, Byelorussian State University, 220080, Minsk, Belarus

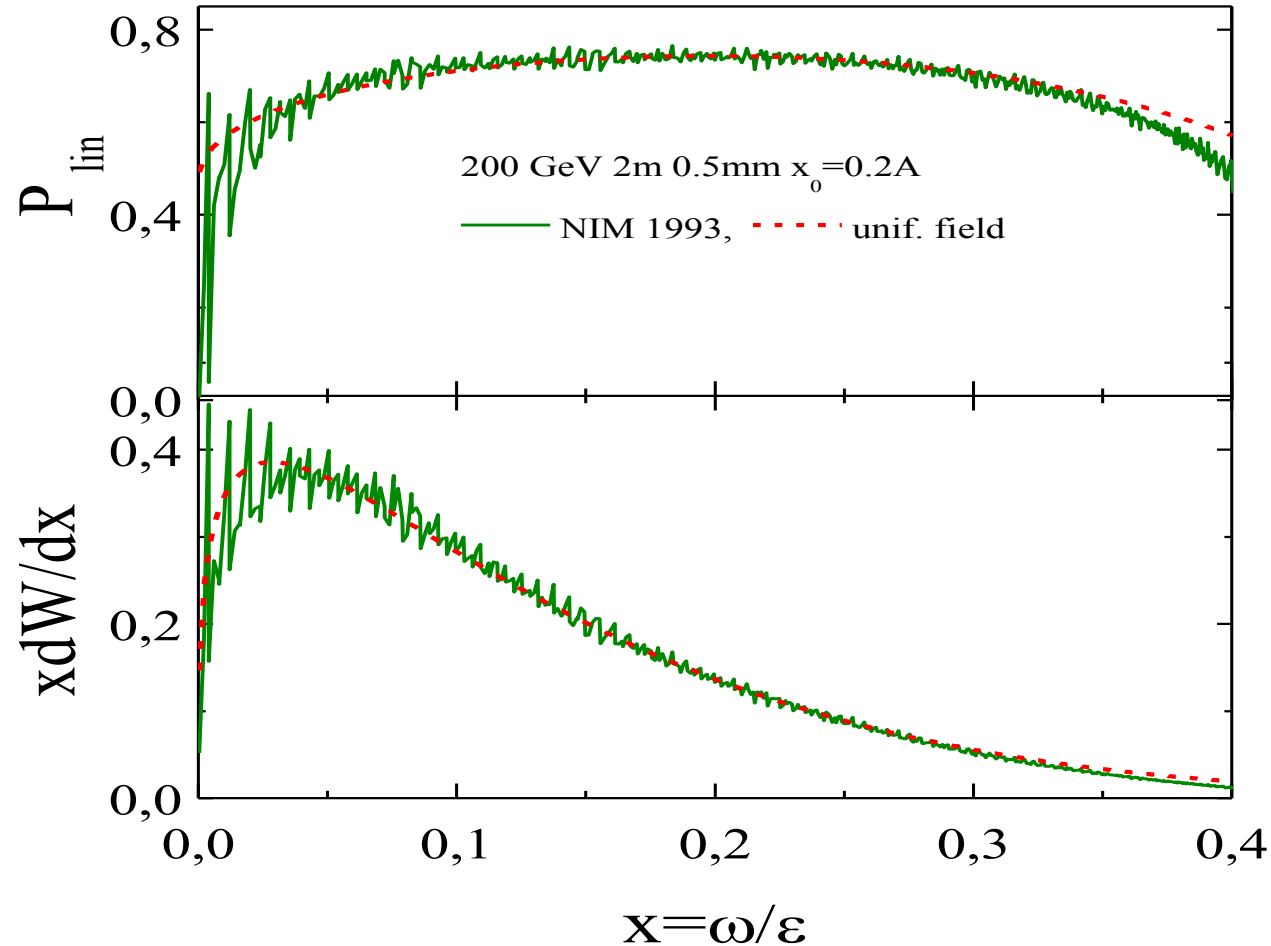
Received 15 March 1992 and in revised form 2 March 1993

A new computational procedure is developed which uses the fast Fourier transform algorithm and allows one to describe the processes of photon emission and pair production at arbitrary angles of high-energy electron, positron and photon propagation relative to the crystal planes.

Polarization and spectrum of 1 GeV channeled e⁺ with channeling radiation contribution



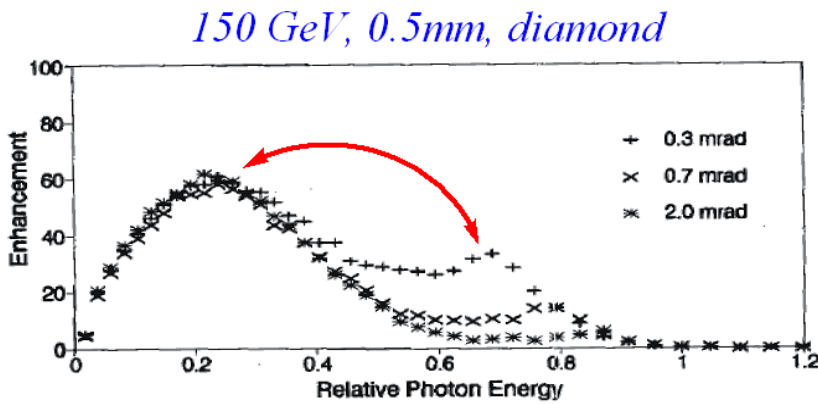
Synchrotron-like approximation at 200 GeV e⁺



The more sophisticated theory:

adding circular polarization to the approach of
 V.N. Baier, V.M. Katkov, V.M. Strakhovenko, NIM B69(1992)258

1. + channeling radiation
2. + circular polarization
3. planar potential \Rightarrow SOS radiation
4. SOS oscillations \Rightarrow channeling radiation



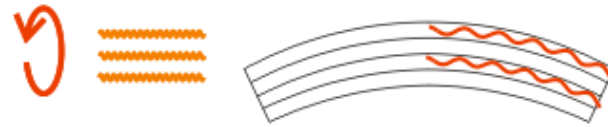
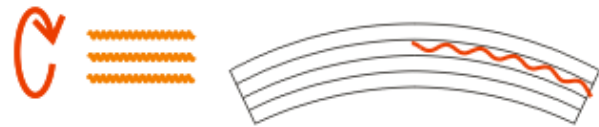
absolutely necessary at $\epsilon \sim 1 \text{ TeV}$

$$\begin{aligned}
 d\omega &= \frac{2\alpha d\omega}{\gamma^2} \sum_{n=1,2,\dots} \frac{e^2 E_n^2}{m^2 q_\parallel^2} \\
 &\times \left\{ (g_1 + \nu) \int_{b_+}^\infty Ai(y) dy - 2g_1 \int_b^\infty Ai(y) dy + (g_1 - \nu) \int_{b_-}^\infty Ai(y) dy \right. \\
 &+ \mu\nu \left(\frac{\chi}{u} \right)^{1/3} [(g_4 + 4\nu g_2) Ai(b_+) - 2\varphi Ai(b)(1 - \Lambda) + (g_4 - 4\nu g_2) Ai(b_-)] \\
 &+ \nu^2 \left(\frac{\chi}{u} \right)^{2/3} [(g_3 - g_2) Ai'(b_+) - 2(g_3 + g_2) Ai'(b) + (g_3 - g_2) Ai'(b_-)] : \\
 d\omega_{12} &= -d\omega_{21} = -\frac{4i\alpha d\omega}{\gamma^2} \sum_{n=1,2,\dots} \frac{e^2 E_{x,n} E_{y,n}}{m^2 q_\parallel^2} \\
 &\times \frac{\varphi}{4} \left\{ (g_5 + \frac{1}{2}) \int_{b_+}^\infty Ai(y) dy - 2g_5 \int_b^\infty Ai(y) dy + (g_5 - \frac{1}{2}) \int_{b_-}^\infty Ai(y) dy \right. \\
 &+ \mu\nu \left(\frac{\chi}{u} \right)^{1/3} [Ai(b_+) - Ai(b_-)] + \frac{1}{4} \nu \left(\frac{\chi}{u} \right)^{2/3} [3Ai'(b_+) - 10Ai'(b) + 3Ai'(b_-)] \Big\}, \\
 b &= (\omega\chi/\varepsilon)^{2/3}(1 + \rho/2), \quad b_\pm = (\omega\chi/\varepsilon)^{2/3}[(1 + \rho/2) \pm 1/\nu], \\
 g_1 &= \frac{\varphi}{4} + \nu^2(1 + \rho/2) - 4\nu^2\mu^2\Lambda, \quad g_2 = [\varphi(1 + \rho/2) - 1]\Lambda, \\
 g_3 &= 1 - 4\varphi\mu^2\Lambda, \quad g_4 = \varphi(1 + \Lambda), \quad g_5 = \nu(1 + \rho/2) + \nu\mu^2, \\
 \mu &= \frac{\chi}{s} = \frac{eE}{2m|q_\parallel|}, \quad \Lambda = \frac{2E_{x,n}^2}{E_n^2}.
 \end{aligned}$$

Incoherent scattering contribution to the local radiation probability

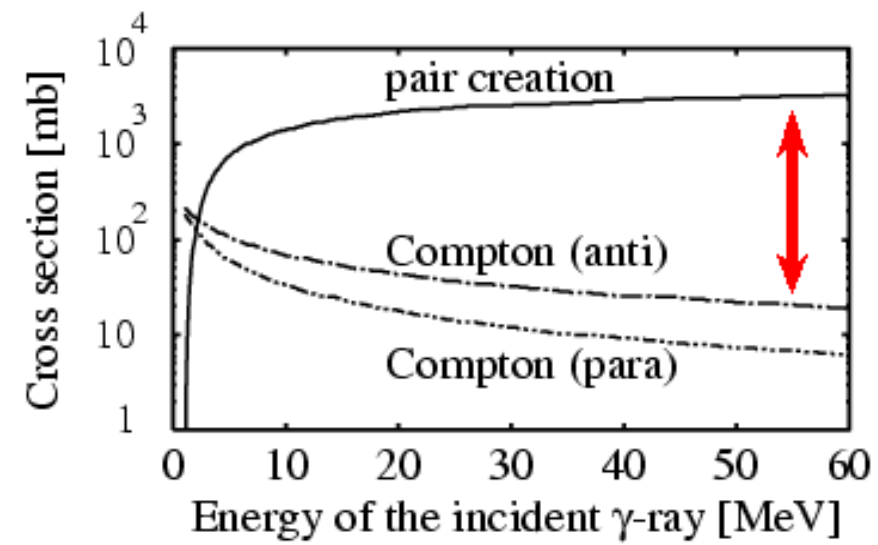
$$d\omega_{inc} = \frac{d\omega}{3L_{rad}\varepsilon^2\omega} \left\{ 2 \left[\varepsilon^2 + \varepsilon'^2 \right] + \omega^2 \right\}$$

Pair production probability dependence on gamma-quantum circular polarization



Essential for
measurement
of gamma

circular polarization
at 100 MeV and above



Probability and polarization asymmetry of channeled positron production

$$\vartheta_x = \theta_x - z/R$$

$$\frac{dw}{d\vartheta_x} = \frac{dw(x)}{d\vartheta_x} = \int \int \frac{d\sigma(\theta)}{d\theta_x d\theta_y} d\theta_y dz = R \int \int \frac{d\sigma(\theta)}{d\theta_x d\theta_y} d\theta_x d\theta_y,$$

$$\begin{aligned} \textcolor{red}{w}(x) &= \frac{1}{2} [w_{xy}(x) + dw_{yx}(x)] = \\ &= \frac{\alpha^2 R}{2\omega} \int_0^\omega \frac{d\varepsilon}{\omega} \sum_{n=1,2,\dots} E_n^2(x) q_{\parallel}^{-2} [\varphi + 4\nu(1-\nu)] \theta(1-\nu) \int_{-\vartheta_x max}^{\vartheta_x max} [1 - P_{dech}(\vartheta_x)] d\vartheta_x \end{aligned}$$

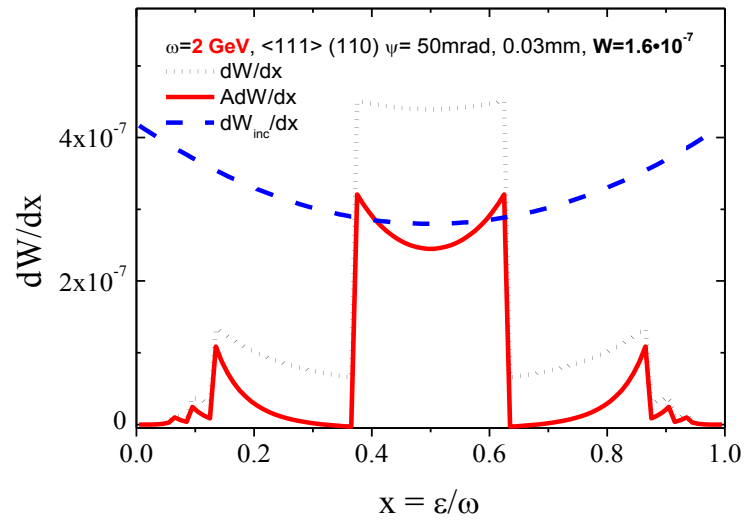
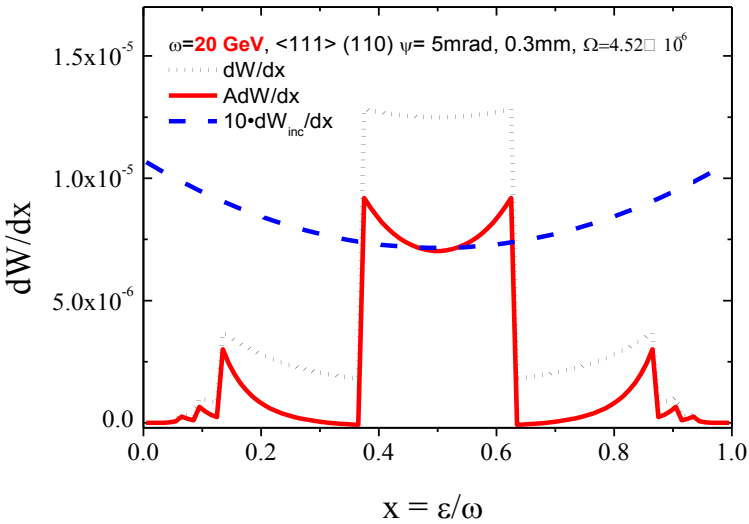
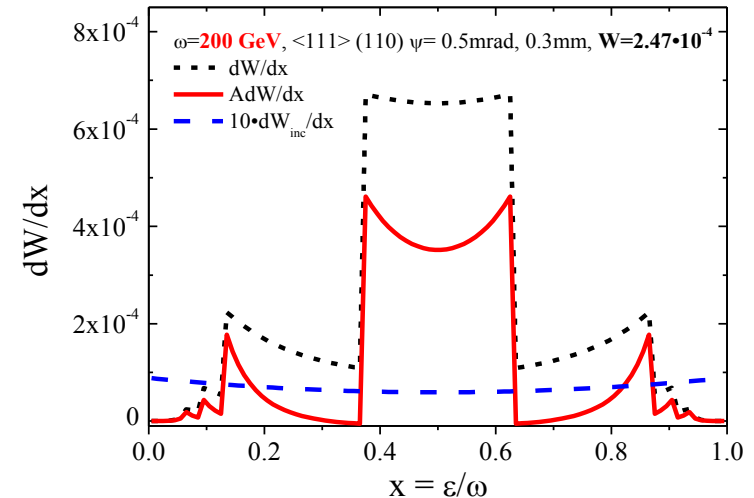
$$\begin{aligned} \textcolor{red}{A}w(x) &= \frac{i}{2} [dw_{xy}(x) - dw_{yx}(x)] = \\ &= \frac{\alpha^2 R}{2\omega} \int_0^\omega \frac{d\varepsilon}{\omega} \sum_{n=1,2,\dots} E_n^2(x) q_{\parallel}^{-2} \xi_2 \varphi (2\nu - 1) \theta(1-\nu) \int_{-\vartheta_x max}^{\vartheta_x max} [1 - P_{dech}(\vartheta_x)] d\vartheta_x, \end{aligned}$$

$$\varepsilon' = \varepsilon - \omega, \quad \varphi = \frac{\varepsilon}{\varepsilon'} + \frac{\varepsilon'}{\varepsilon}, \quad \nu = \frac{\omega m^2}{2\varepsilon \varepsilon' q_{\parallel}}, \quad q_{\parallel} = n q_{1y} \psi v$$

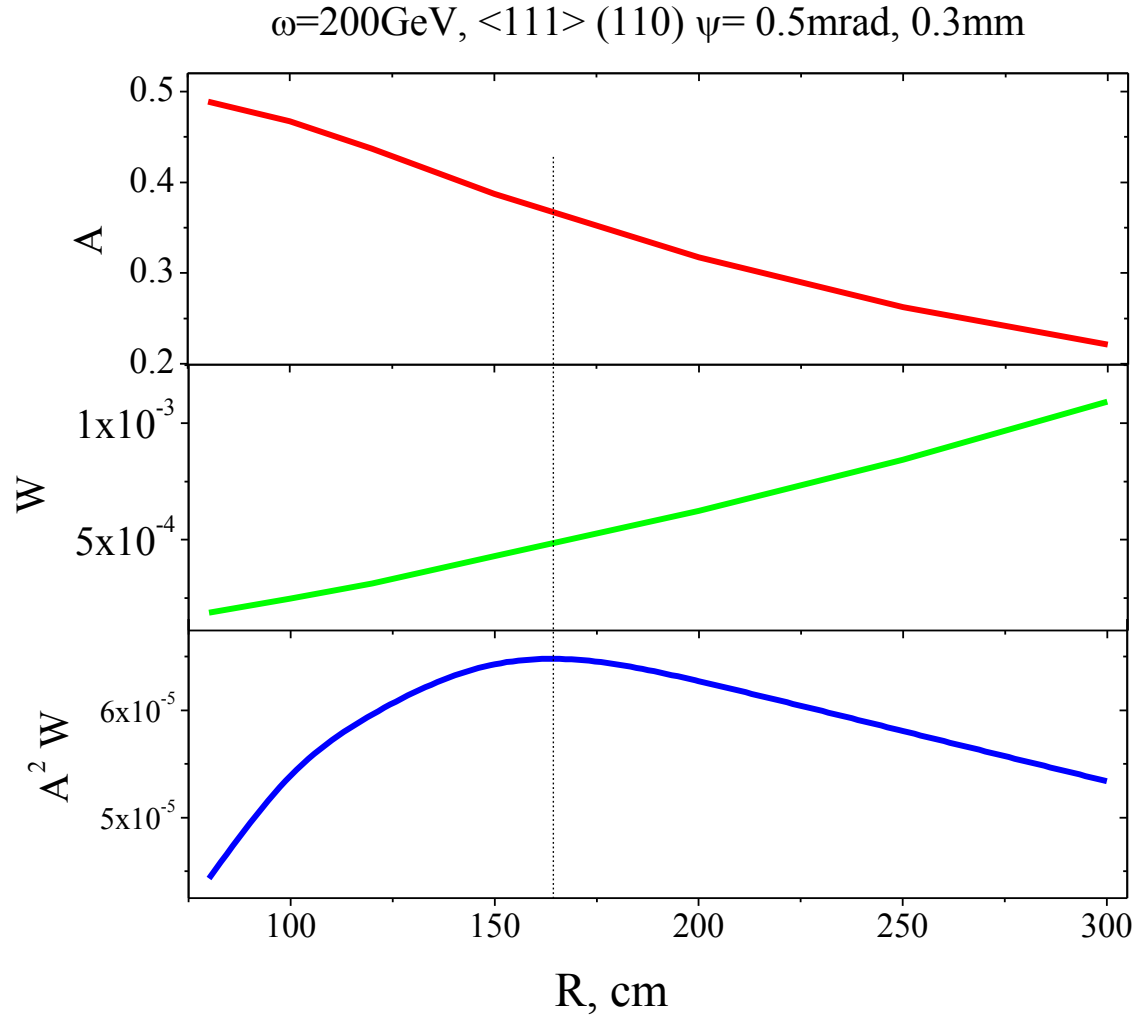
are expressed through values integrated over both transverse angles

Differential pair production probability and polarization asymmetry

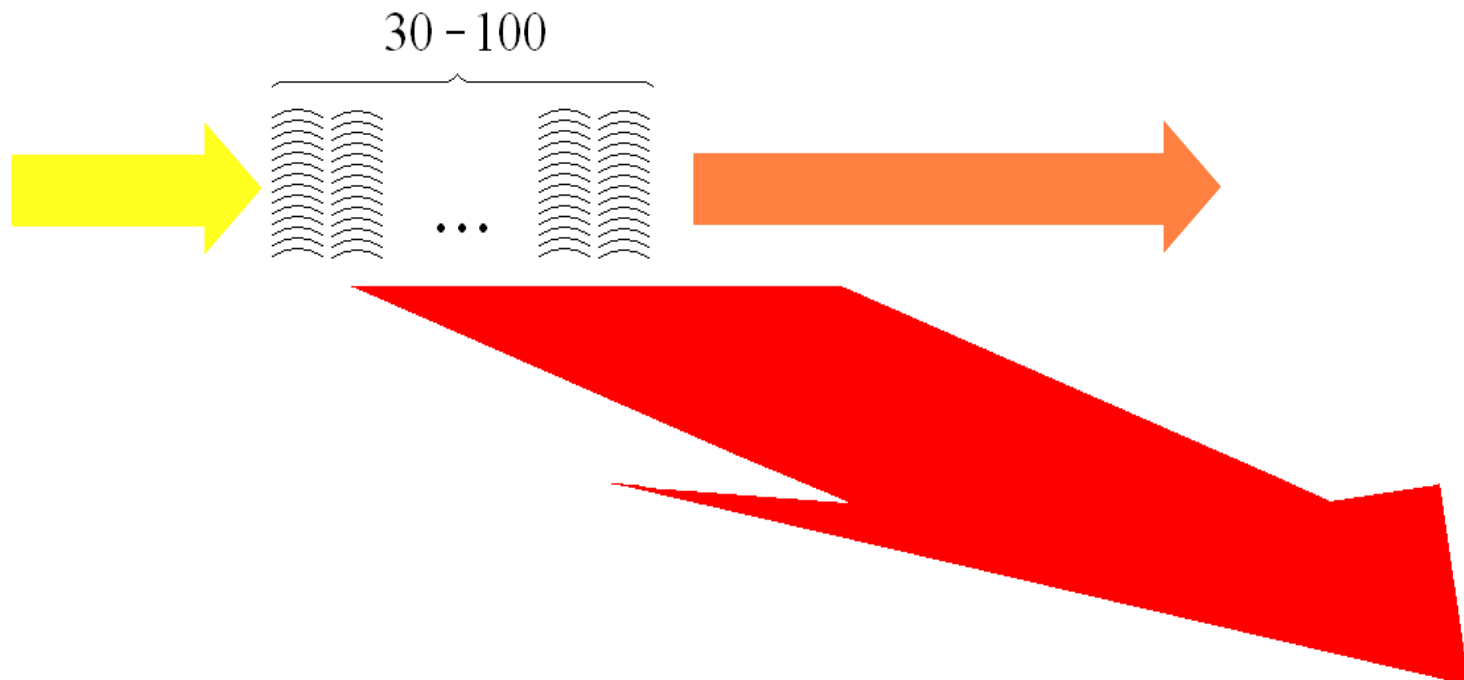
at 2, 20 and 200 GeV



Bending radius optimization at 200 GeV



Tens of crystal can be used for gamma CP measurements

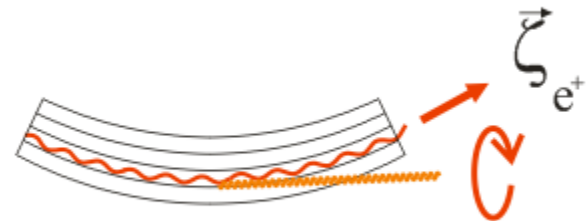
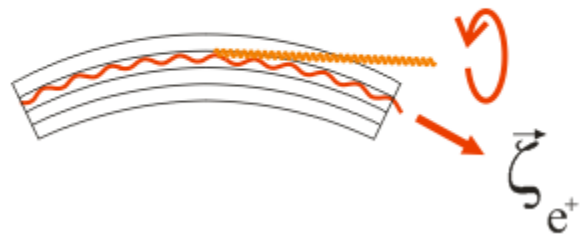


$W(\hbar)$

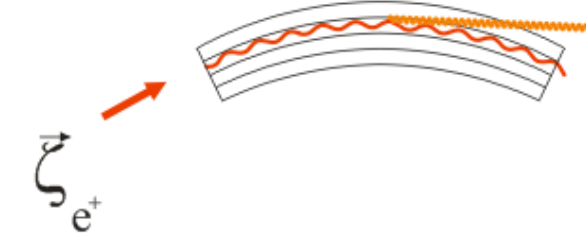
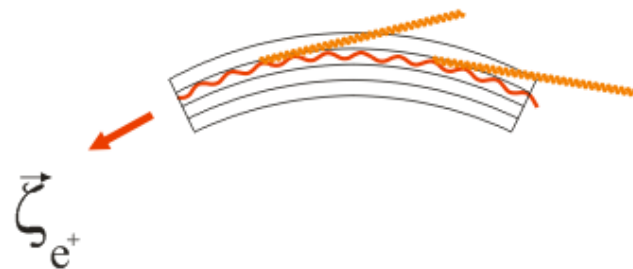
\hbar

\hbar

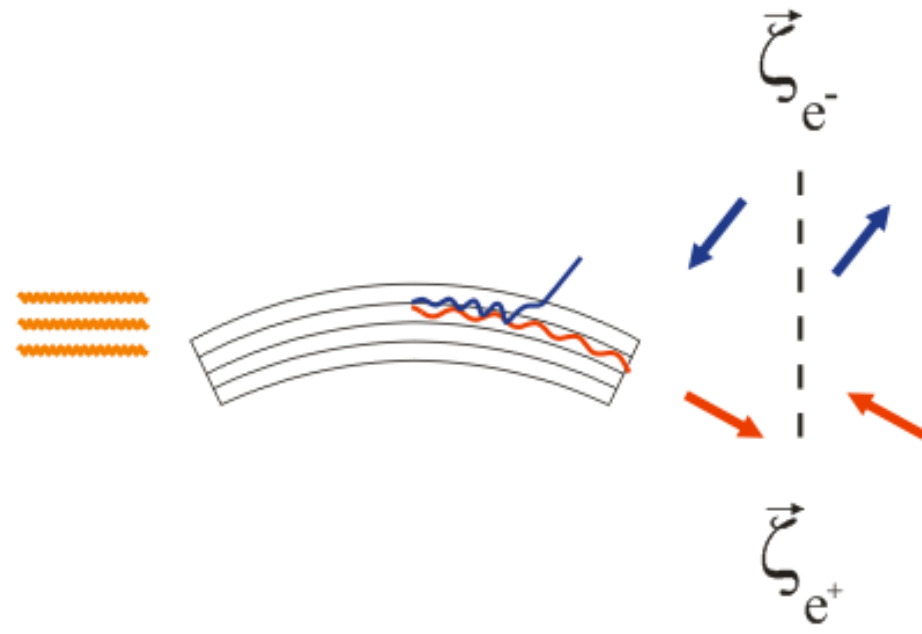
Positrons become longitudinally polarized after circularly polarized gamma-quanta emission



Longitudinal positron polarization can be measured



Longitudinally polarized *electrons*
can be produced

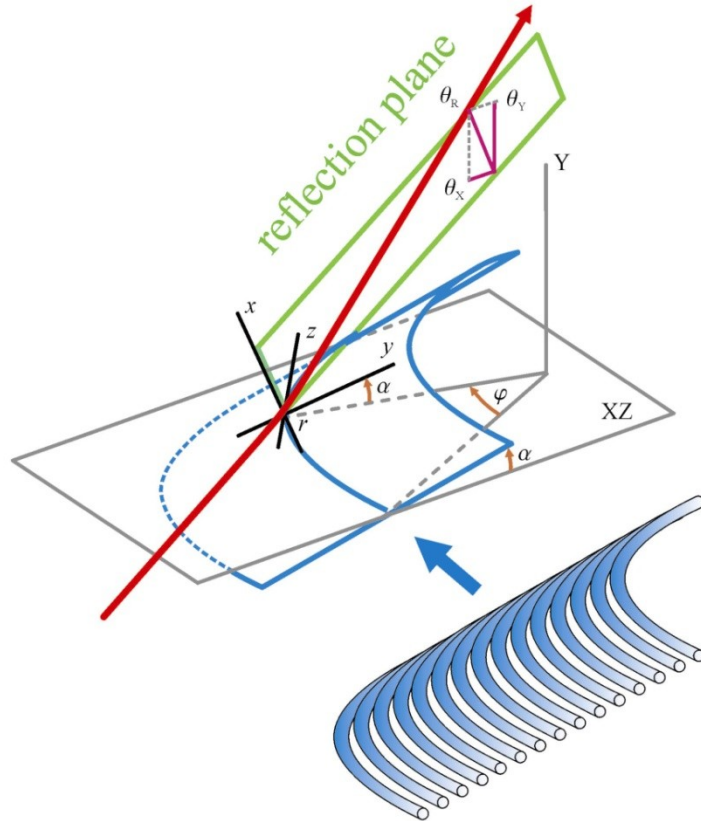
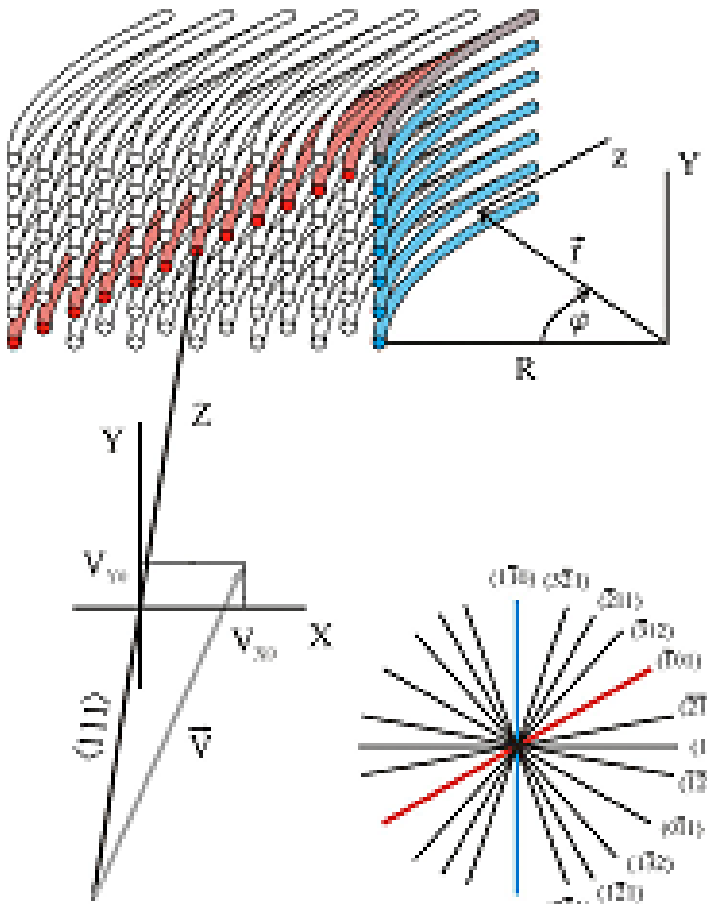


Conclusions for CPCB

- Hard string-of-string radiation peak is highly circularly polarized
- Circular gamma-quantum polarization can be measured in a new way
- Both effects are observable at 1 GeV and above

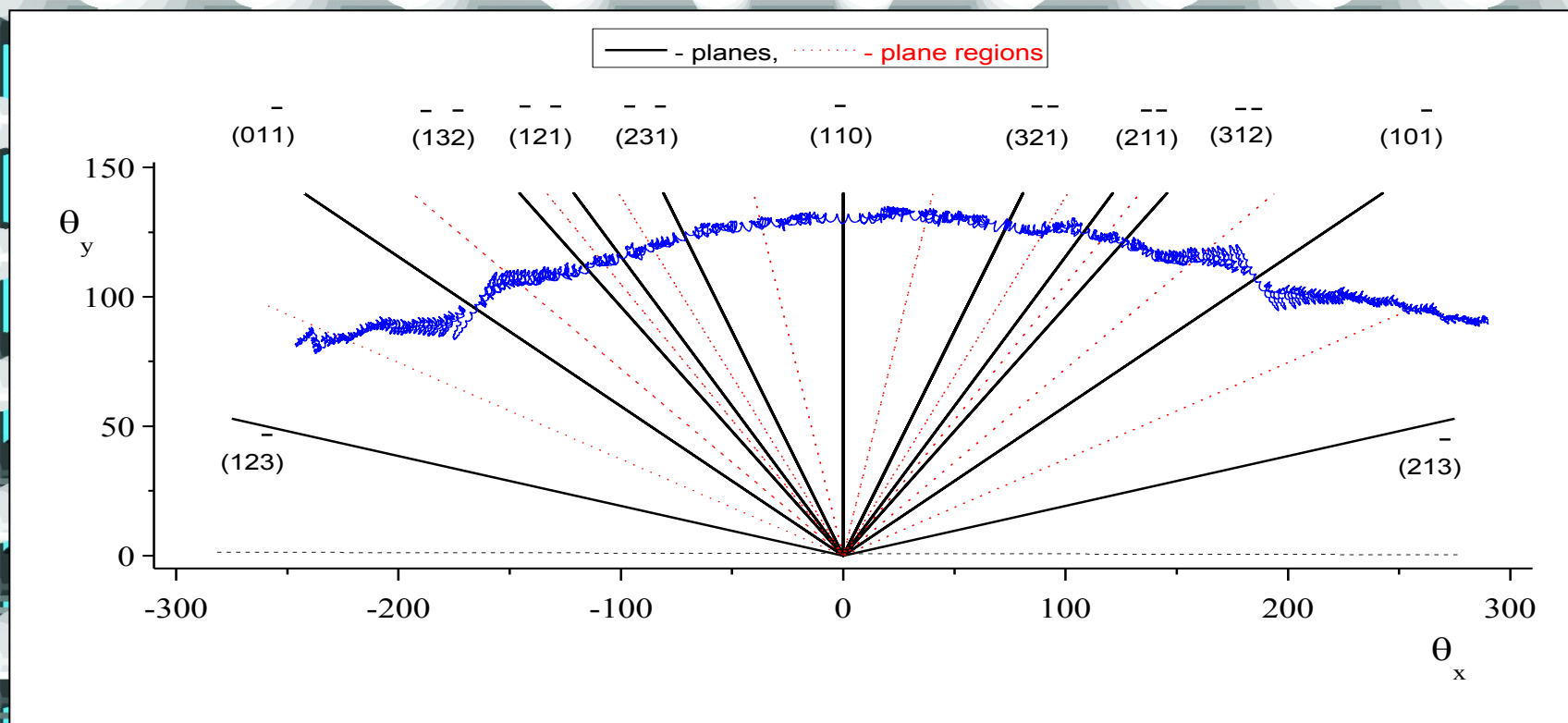
Multiple Volume Reflection in One Crystal (MVROC)

V.V. Tikhomirov, PLB 655(2007)217

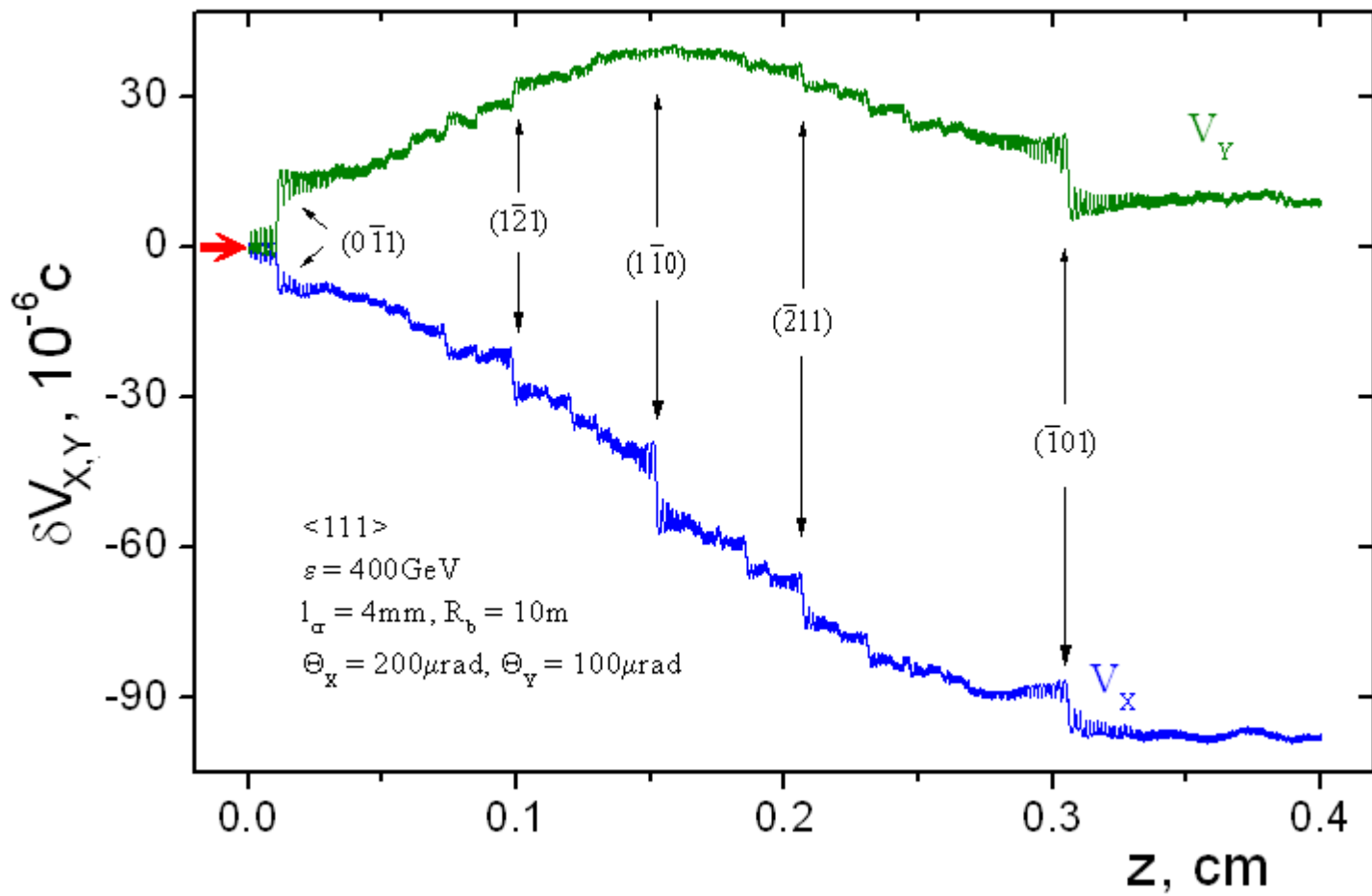


Axes form *many* inclined reflecting planes

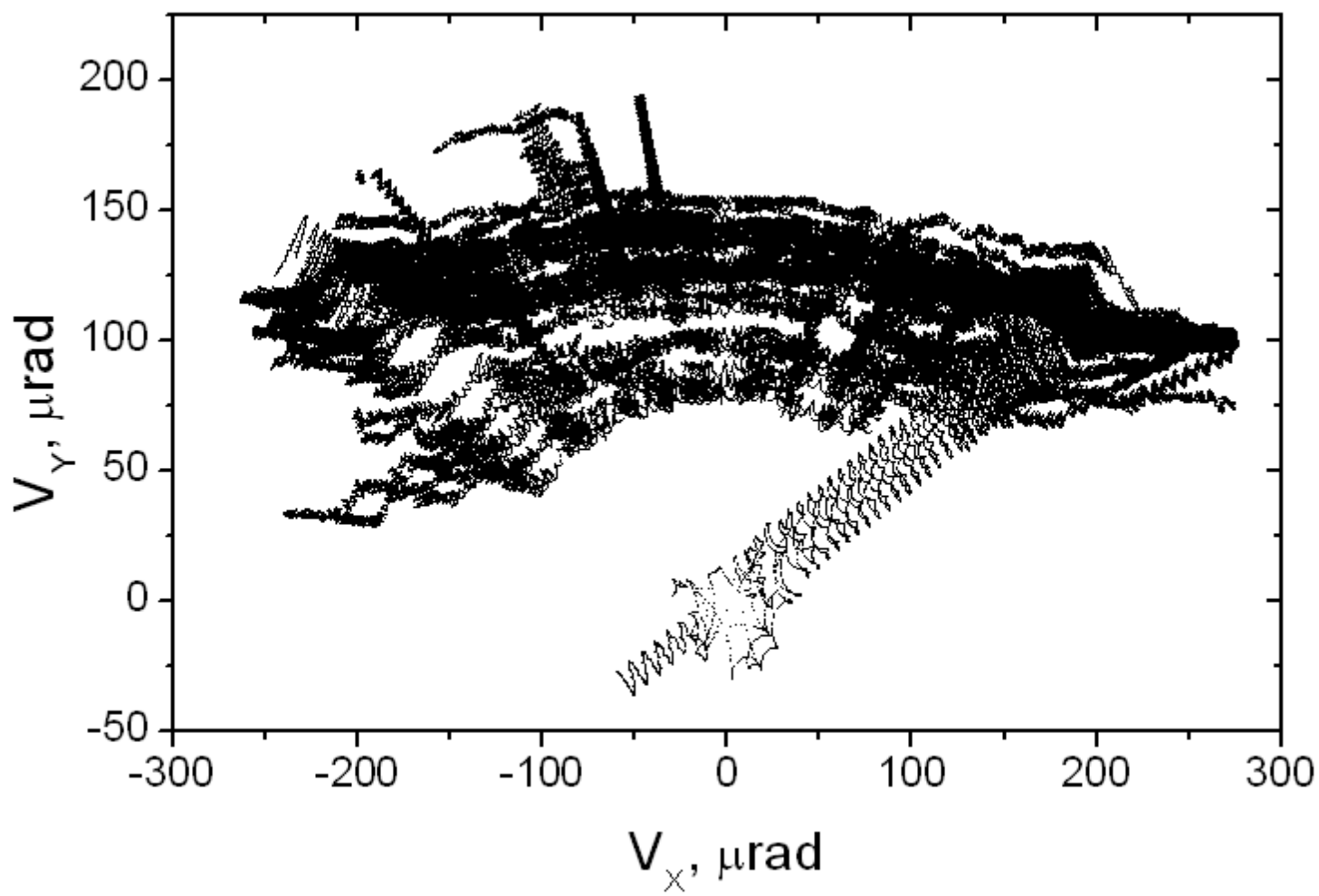
Planes intersecting along $\langle 111 \rangle$ axis, the plane influence angular regions and a positron trajectory



A positron trajectory

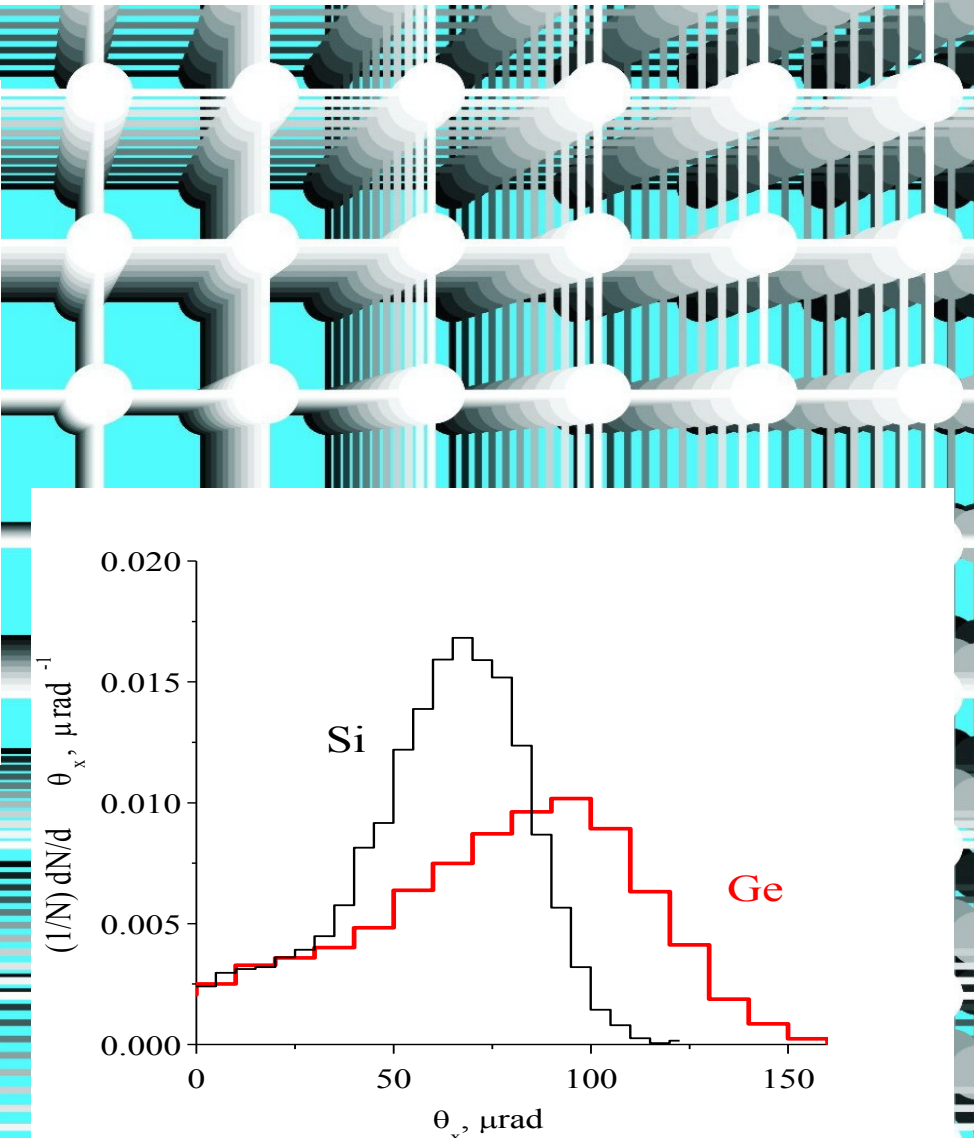
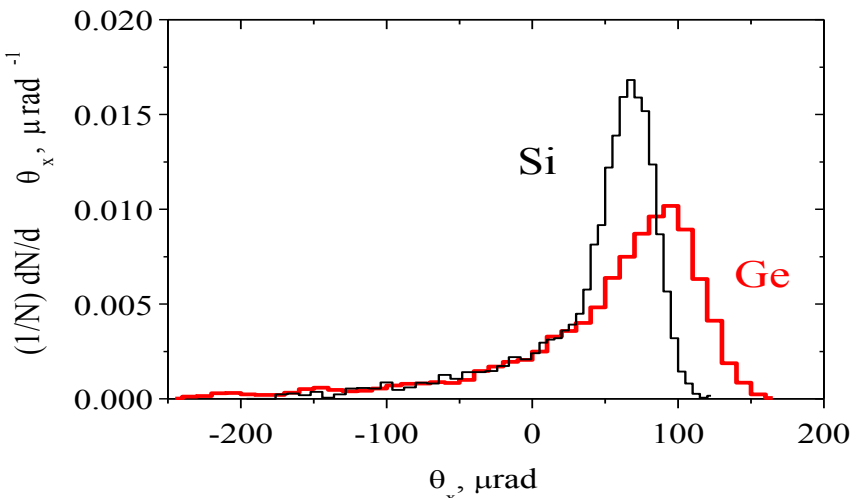


Positron trajectories



Volume reflection angle increase in Ge

Ge <111> 400 GeV 4mm 11.43/1.35m Vx=195*1.35 Vy=85*1.35
dvx=11, dvy=9.136 77.07/51.9
Si <111> 400 GeV Gaussian asymmetric, $\delta\theta_x = 11\mu\text{rad}$, $\delta\theta_y = 9.13\mu\text{rad}$,
 $\theta_x = 195\mu\text{rad}$, $\theta_y = 85\mu\text{rad}$



A new method to calculate the characteristics of radiation and pair production under high energies and arbitrary angles of particle incidence relative to the crystal planes

V.V. Tikhomirov

Institute of Nuclear Problems, Byelorussian State University, 220080, Minsk, Belarus

Received 15 March 1992 and in revised form 2 March 1993

A new computational procedure is developed which uses the fast Fourier transform algorithm and allows one to describe the processes of photon emission and pair production at arbitrary angles of high-energy electron, positron and photon propagation relative to the crystal planes.

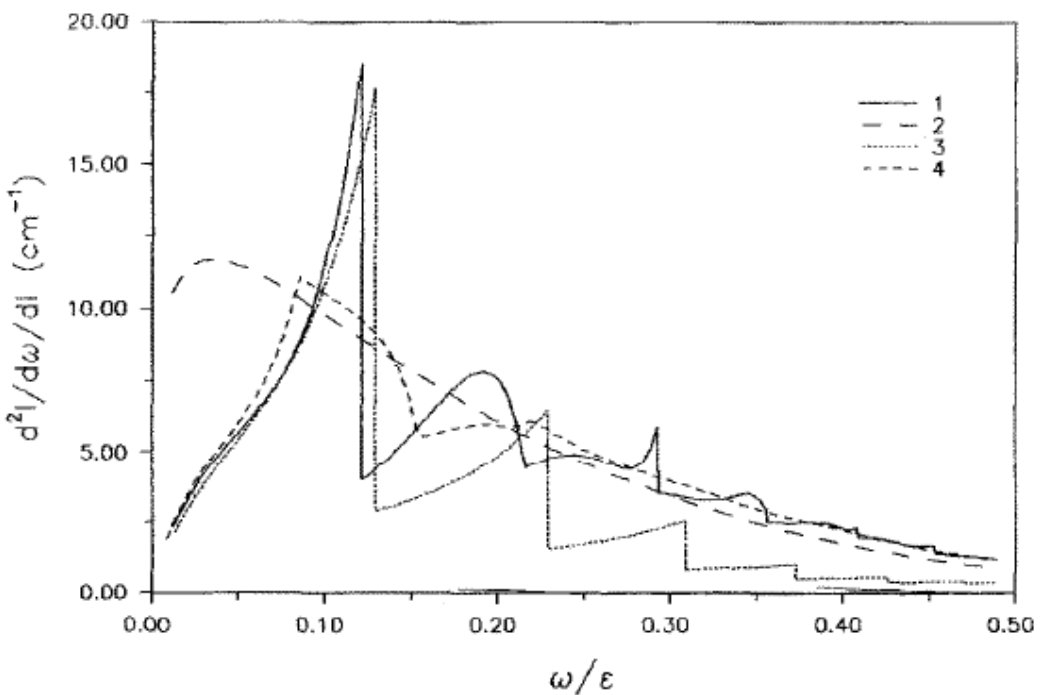


Fig. 1. The radiative power spectra of 150 GeV positrons moving at a tilt angle of 30 μrad relative to the (110) plane of Ge crystal at $T = 293$ K. Curves 1, 2, and 3 are, respectively, the predictions of eqs. (13) and (14), of the uniform field approximation and of the modified coherent bremsstrahlung theory. Curve 4 is obtained using eq. (13) averaged over the uniform tilt angle distribution in the interval 25–35 μrad . Curves 1 and 4 are evaluated using eqs. (13) and (14) and the fast Fourier transform algorithm.

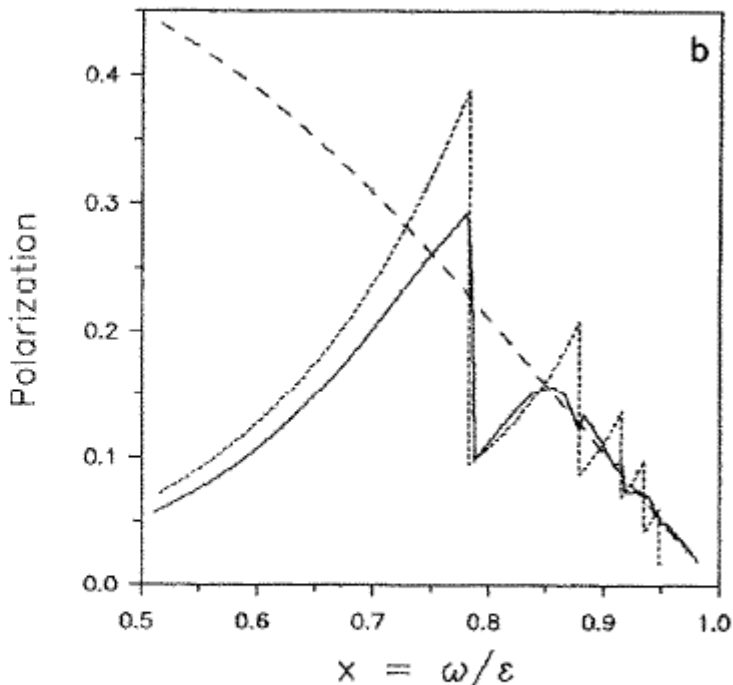
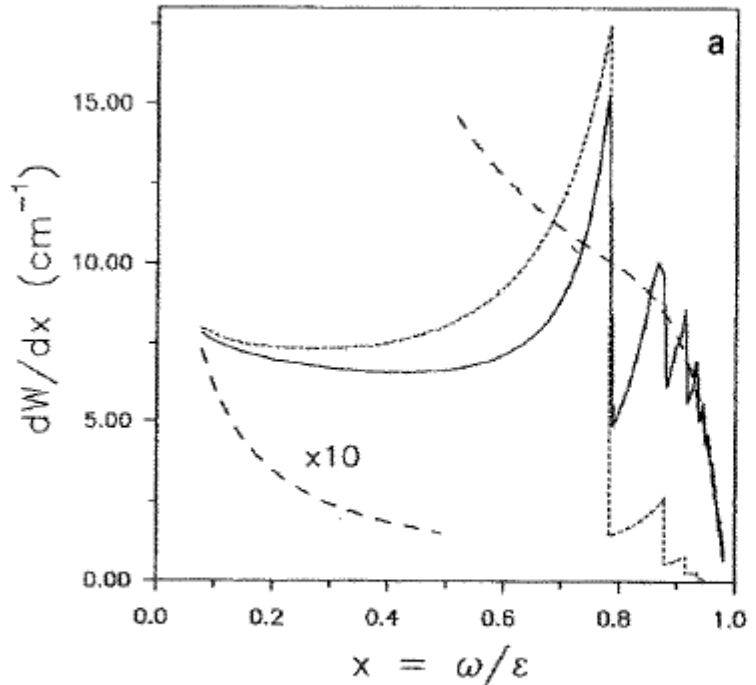


Fig. 3. Spectrum (a) and polarization (b) of radiation of 10 TeV e^- , moving at tilt angle of 12 μrad relative to the (110) plane of diamond. Solid, dashed and dotted curves are, respectively, the predictions of eqs. (13) and (14), of the uniform field approximation and of the modified coherent bremsstrahlung theory. Solid curves are evaluated using the FFT algorithm.

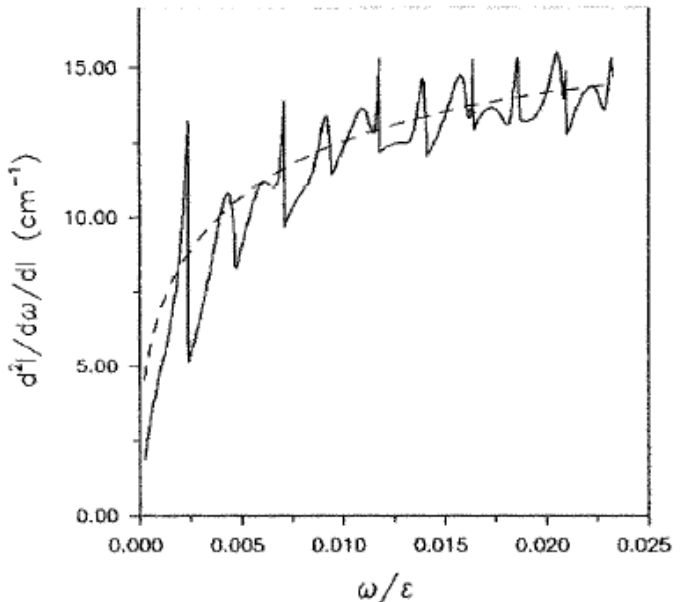


Fig. 2. The radiative power spectra of channeled 150 GeV positrons moving with the transverse energy $\epsilon_{\perp} = V_{\max} - 1$ eV in the field of the Ge (110) planes at 293 K. V_{\max} is the maximum value of the continuum planar potential. The solid and dashed curves are, respectively, the predictions of eqs. (13) and (14) obtained using the FFT algorithm and those of a uniform field approximation.

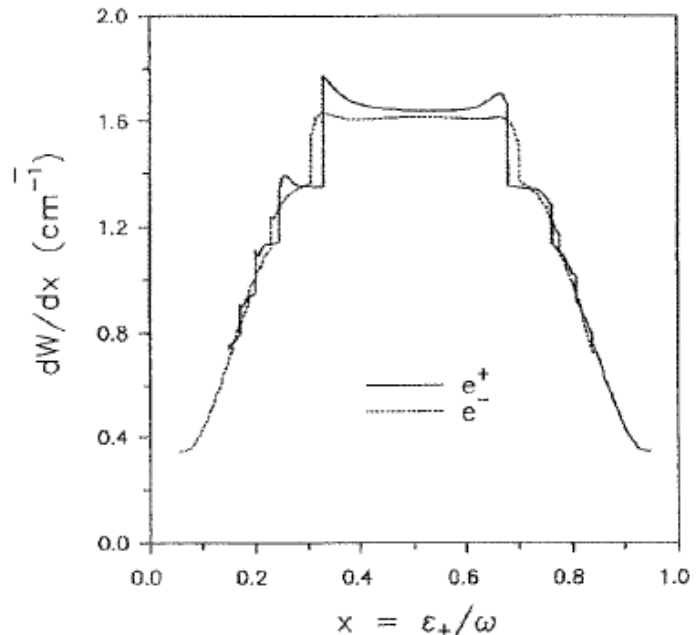


Fig. 4. Pair production probability differentiated with respect to e^+ energy evaluated by the semiclassical formulas written in terms of e^+ (solid curve) and e^- (dotted curve) trajectories, respectively, using the FFT algorithm in the case of 1 TeV photons having the tilt angle of $30 \mu\text{rad}$ relative to the (110) plane of Ge crystal at 293 K.

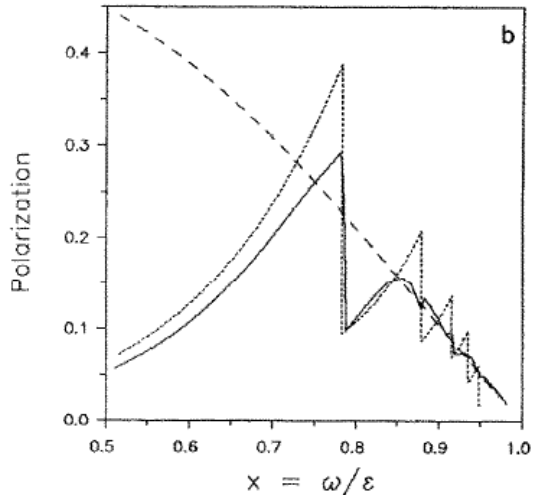
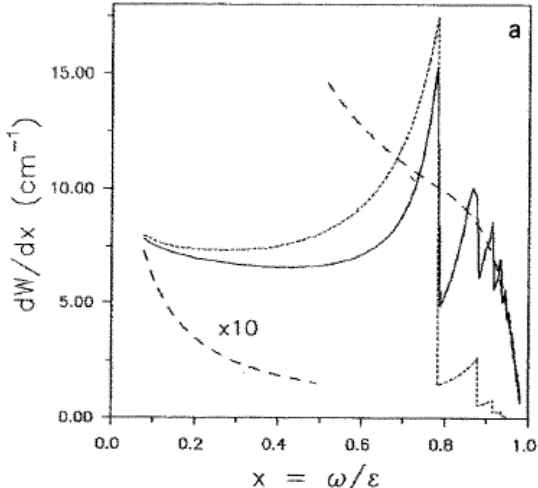


Fig. 3. Spectrum (a) and polarization (b) of radiation of 10 TeV e^- , moving at tilt angle of 12 μrad relative to the (110) plane of diamond. Solid, dashed and dotted curves are, respectively, the predictions of eqs. (13) and (14), of the uniform field approximation and of the modified coherent bremsstrahlung theory. Solid curves are evaluated using the FFT algorithm.

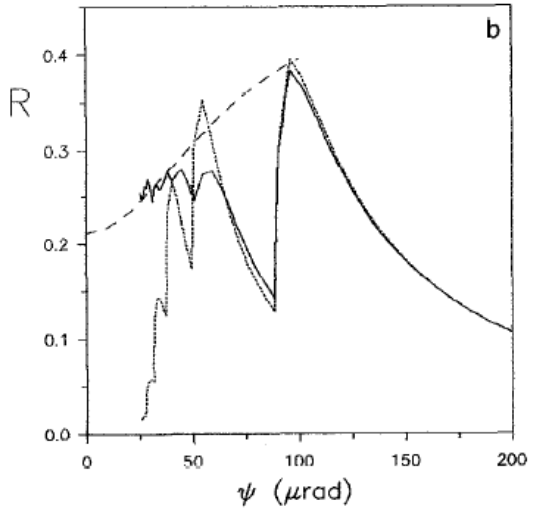
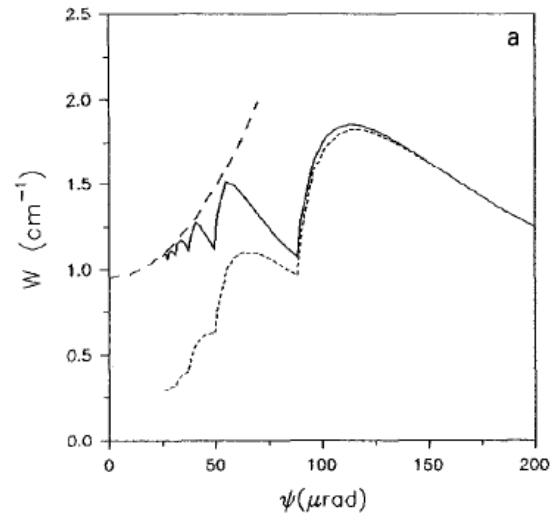
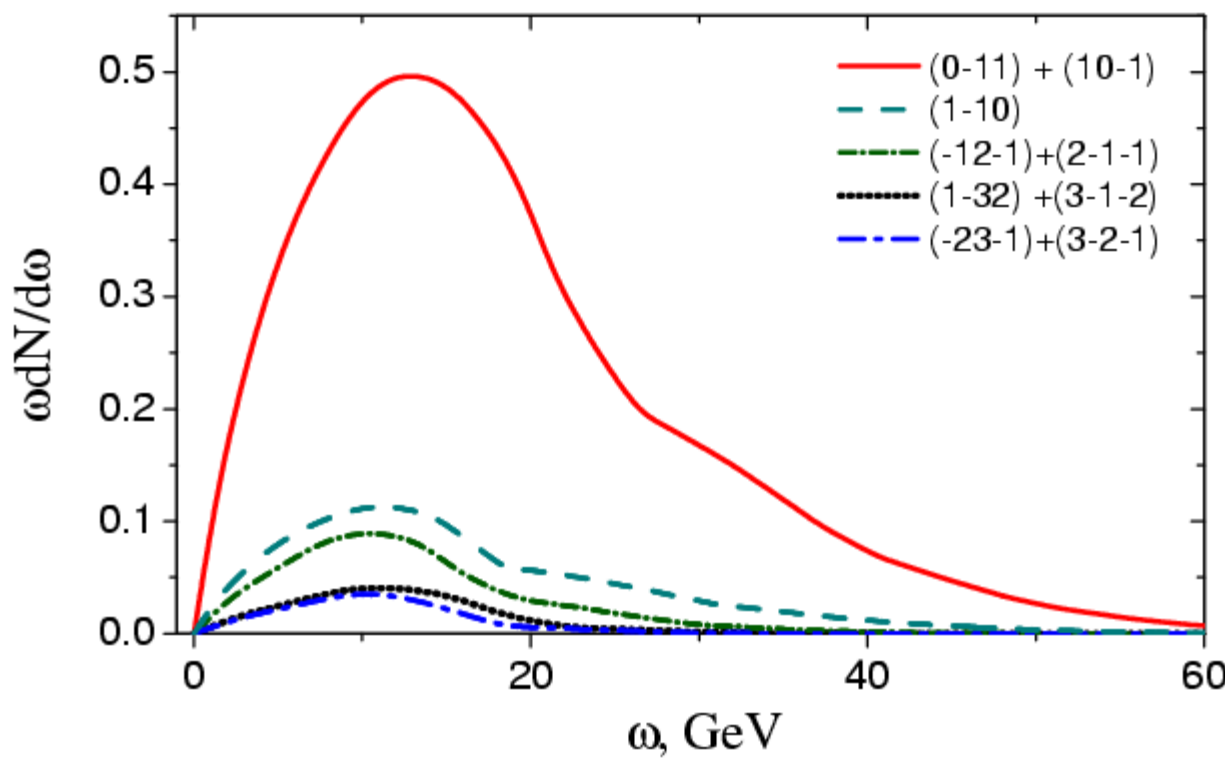
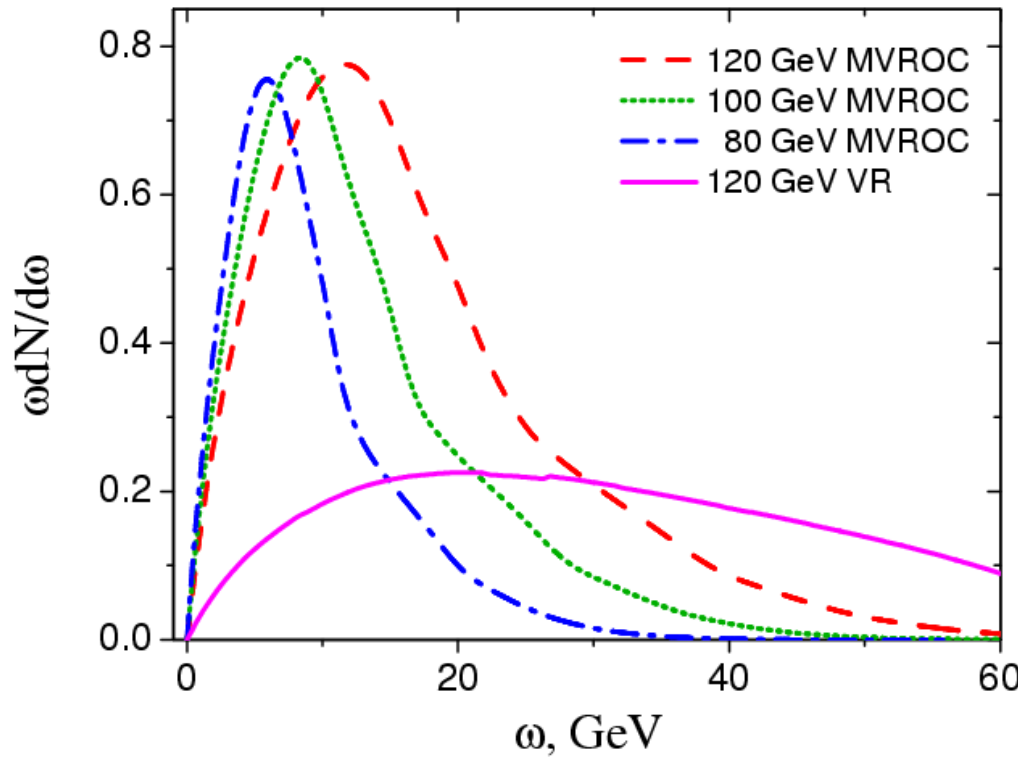


Fig. 5. Integral probability of pair production by unpolarized 1 TeV photons in Ge crystal at 293 K (a) and asymmetry ratio (19) of pair production by polarized photons (b) as a function of their tilt angle relative to the (110) plane. The dashed, dotted and solid curves are obtained using, respectively, the correction [10,11] to the uniform field approximation, the modified theory of coherent pair production [2,11] and the semiclassical formula used along with the FFT algorithm.

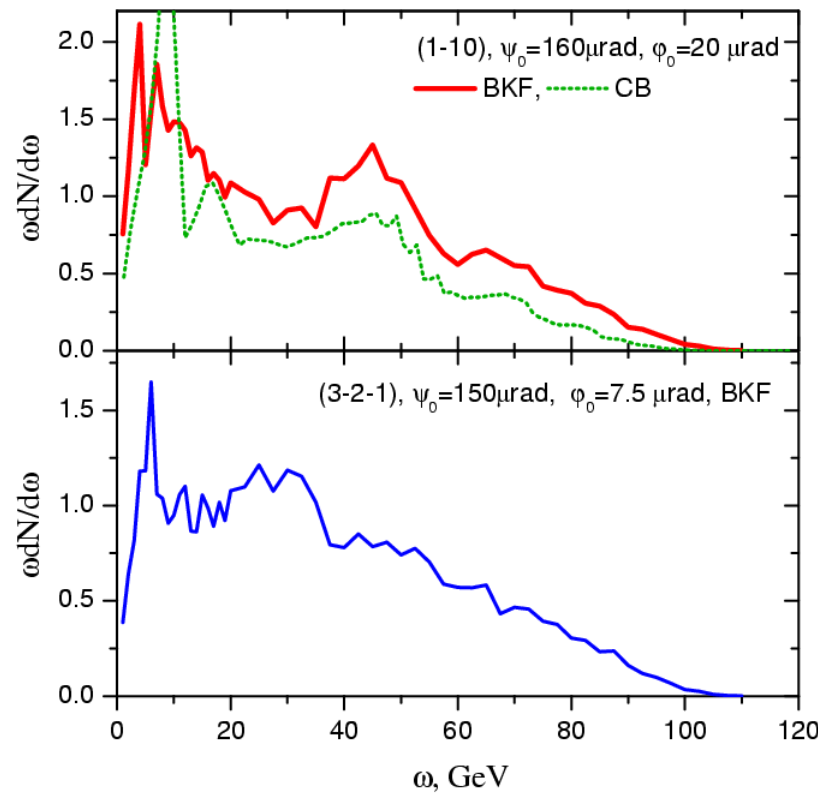
Contribution of different plane sets to 120 GeV e^+ radiation spectral intensity



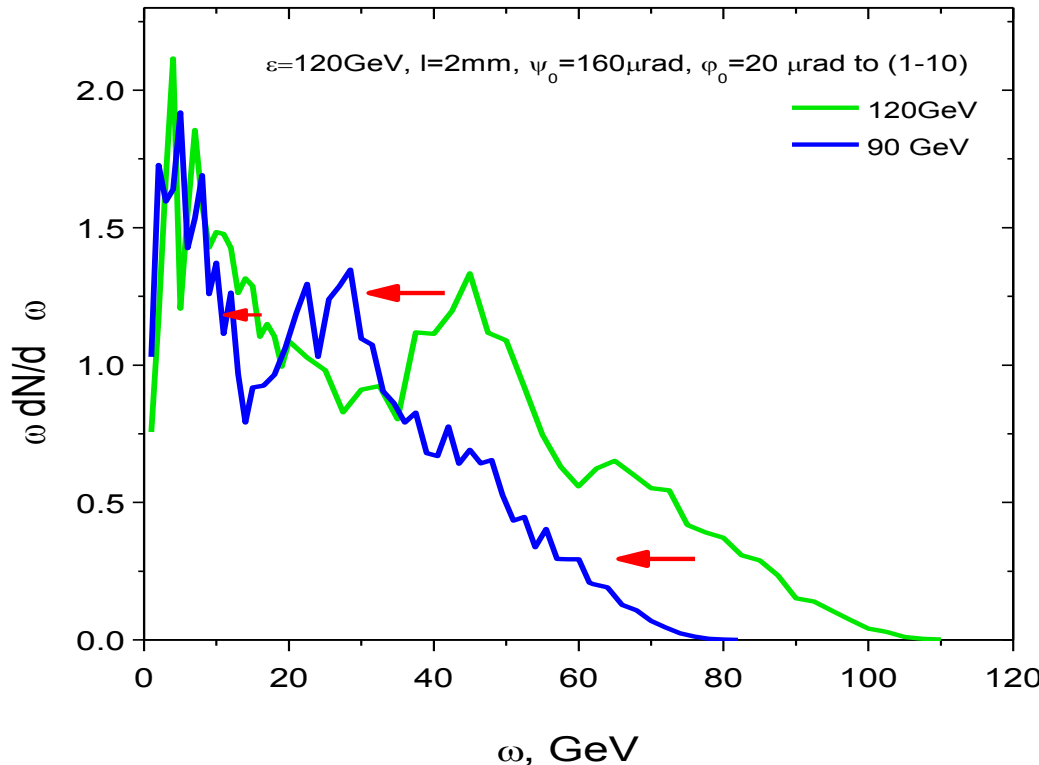
Spectra of radiation of 120, 100 and 80 GeV positrons in MVROC conditions and of 120 GeV positrons in VR conditions, all in 2mm Si crystal bent with radius of 4.7 m.



Spectra of energy radiated by 120 GeV positrons in the 2mm Si crystal in the field of (110) (up) and (321) (down) planes. CB theory predictions are also shown for the former by dotted line.

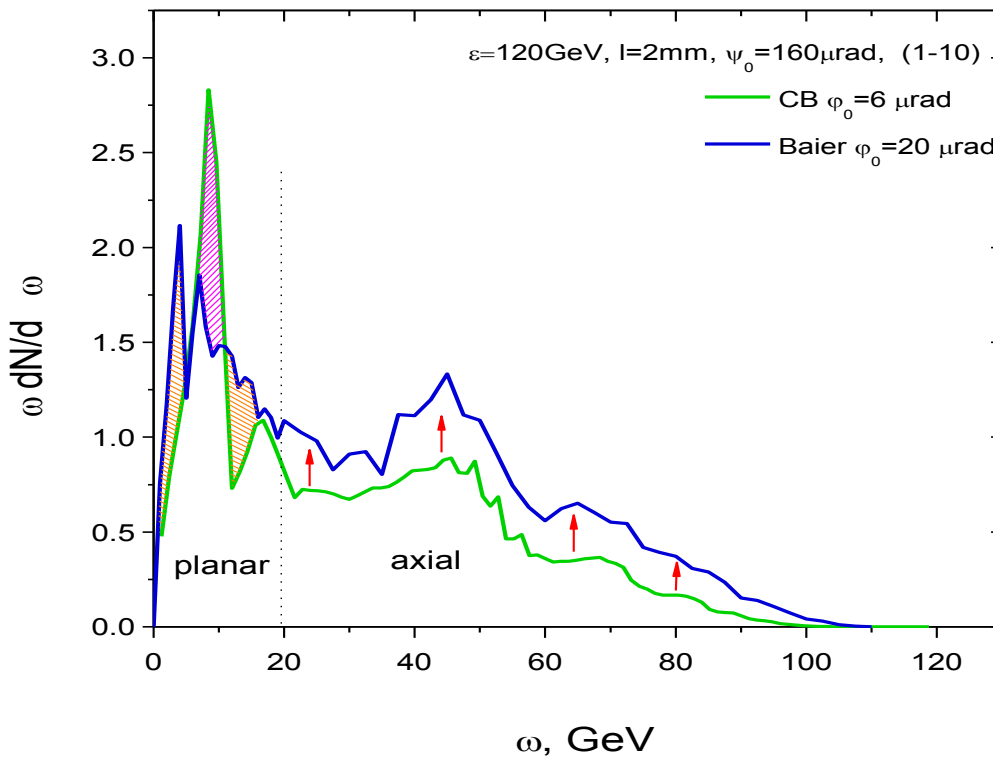


Spectrum evolution with positron energy



All types of radiation becomes softer

CB theory applicability

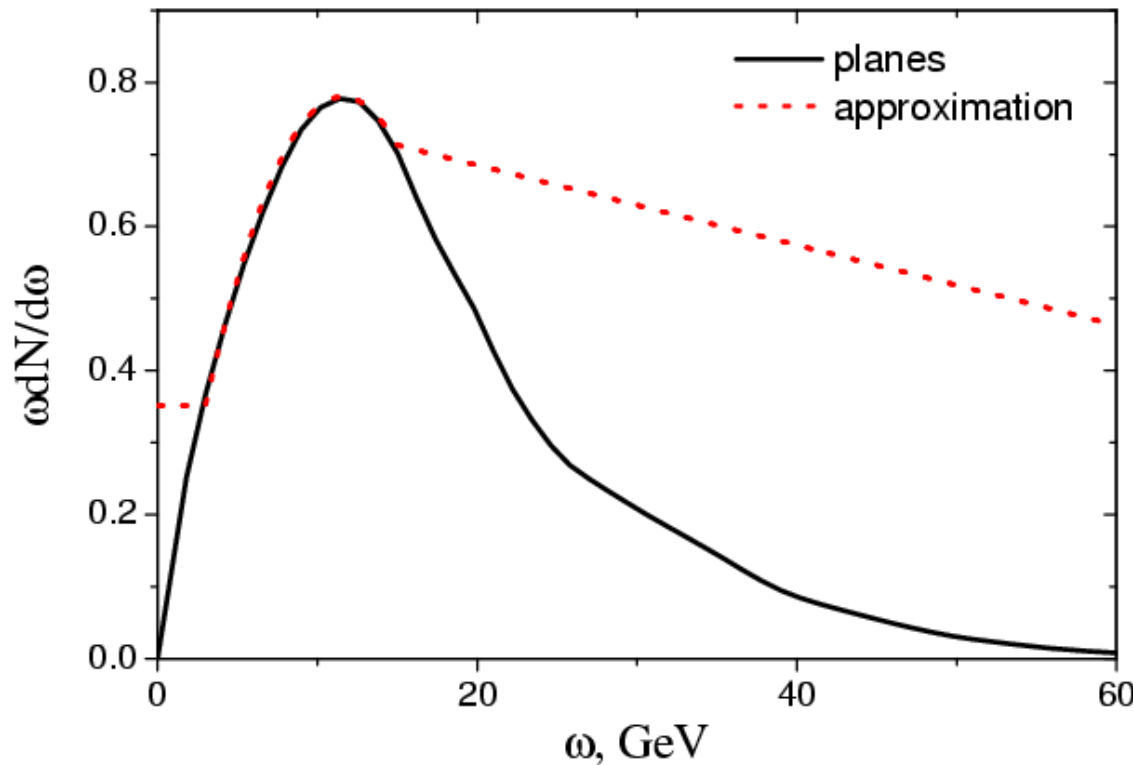


axial radiation
planar radiation

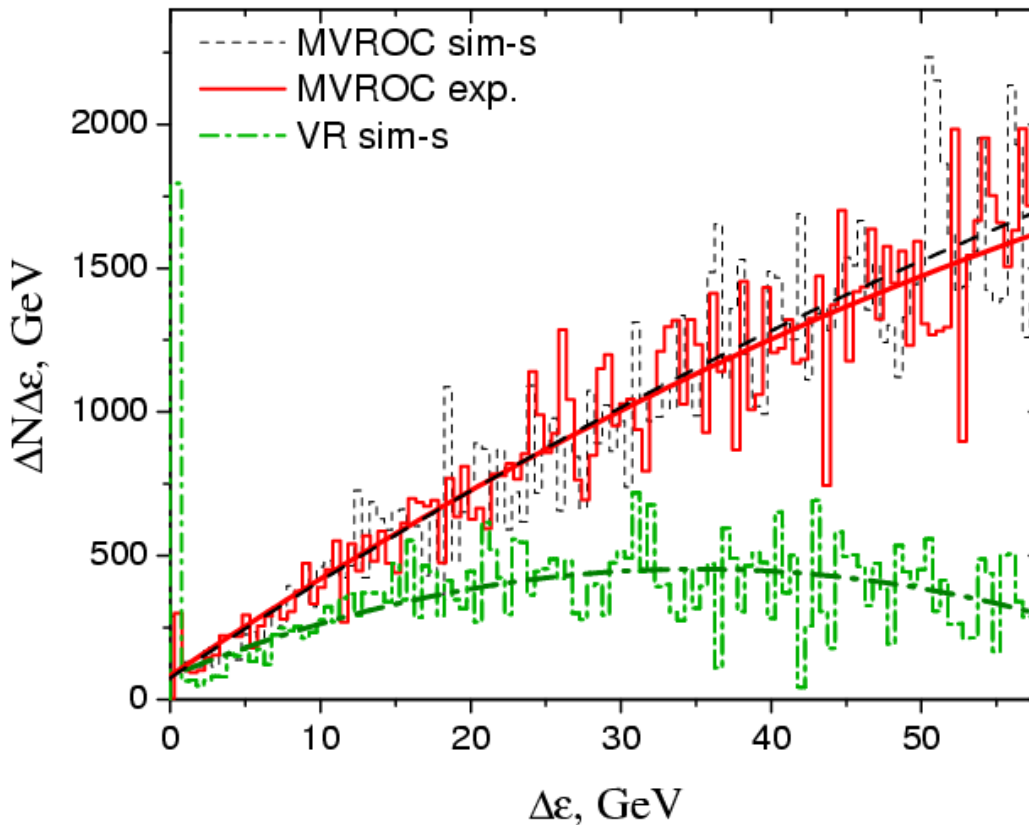
is underestimated
perhaps no

Are there hopes for simplified theory?

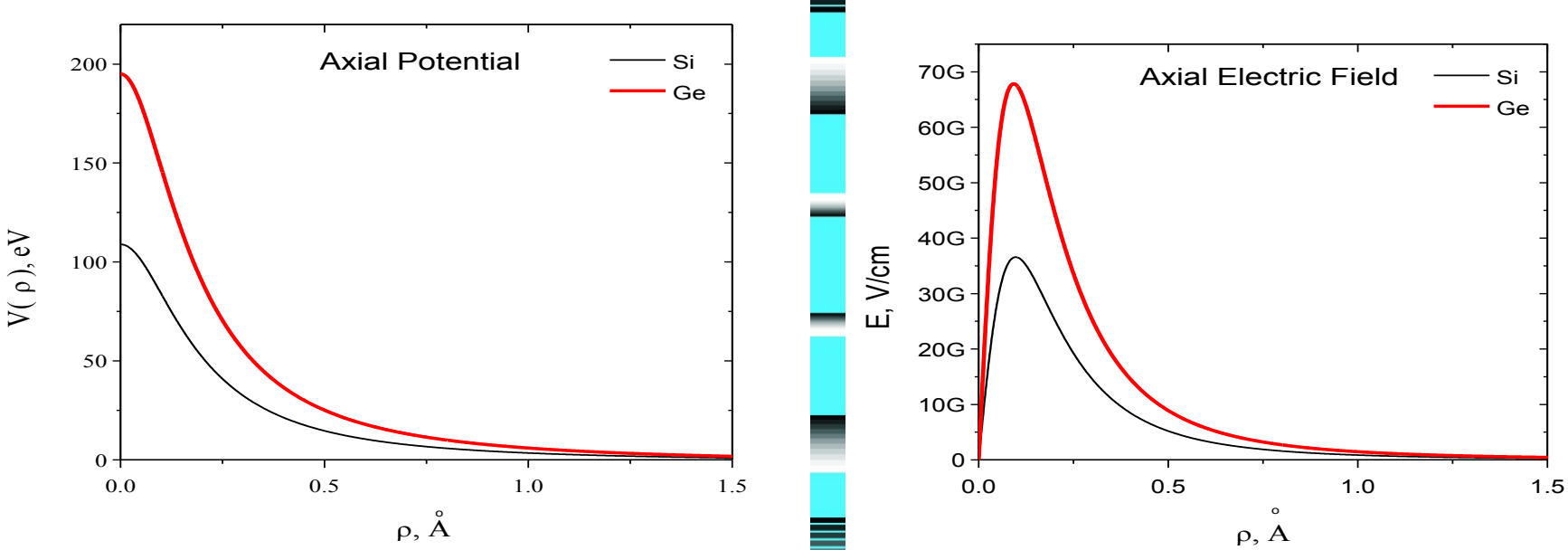
Modification of the planar radiation spectrum used to reproduced the experimental positron energy loss distribution



Experimental positron MVROC energy loss spectrum (solid), simulated MVROC (dashed) and VR (dash-dotted) energy loss spectra. Polynomial interpolations are also shown by the same types of lines.



Comparison of axial potential and field strength in Si and Ge



Both potential and field strength are nearly **twice as large** in Si than in Ge

Comparison averaged potentials and field strengths of Ge and Si planes and axes

		Si(293K)	Ge(293K)		Ge(100K)	
<110>	V_0 , eV	133	229	172%	309	232%
<110>	E_{\max} , GV/cm	46	78	170%	144	313%
		Si(293K)	Ge(293K)		Ge(0K)	
(110)	V_0 , eV	21.5	37.7	175%	44.0	205%
(110)	E_{\max} , GV/cm	5.7	9.9	1.74	14.9	261%

$u(293K)=0.085\text{\AA}$, $u(100K)=0.054\text{\AA}$, $u(0K)=0.036\text{\AA}$

Ge cooling is very productive!

Investigating Strong Field QED effects

$$\chi = \frac{E}{1.32 \cdot 10^{16} eV/cm} \frac{\epsilon}{mc^2}$$
 - the main parameter of quantum electrodynamics

		Si(293K)	Ge(293K)	Ge(100K)
<110>	E _{max} , GV/cm	46	78	170%
	χ(120GeV)	0.82	1.39	2.56

$$I(\chi \ll 1) \propto E^2,$$
$$I(\chi \sim 1) \propto E,$$
$$I(\chi \gg 1) \propto E^{2/3}$$

Radiation intensity will grow like $E \div E^2$

Manifestation of e^+e^- pair production in semi-uniform field crystal field

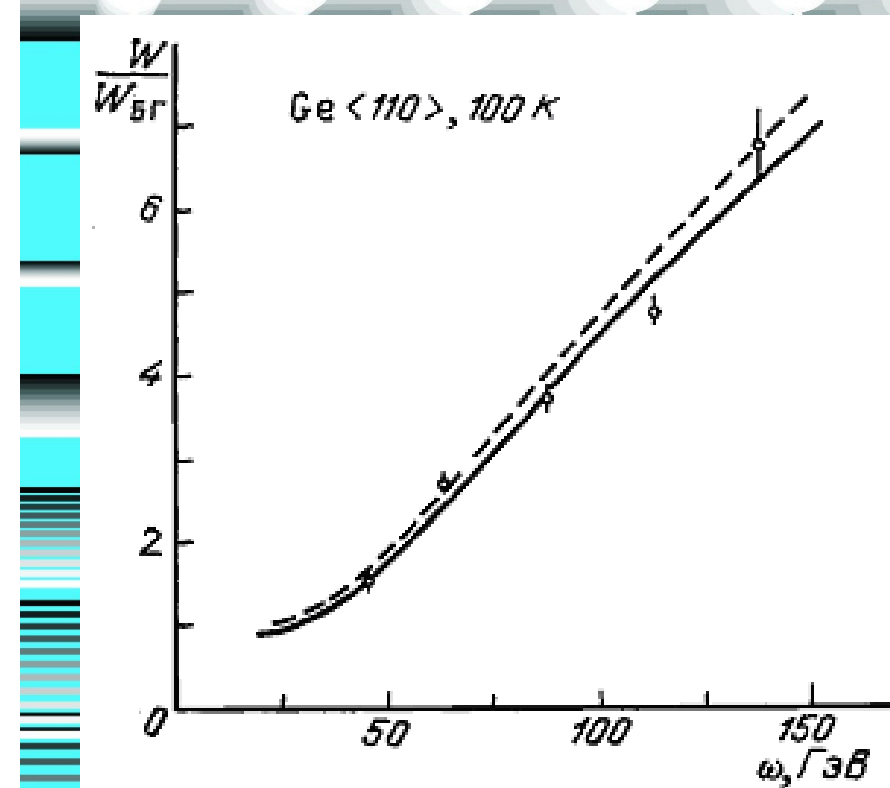
Baryshevskii V.G., Tikhomirov V.V.

Phys. Lett. 90A(1982); Yad. Fiz. 36(1982)697.

Energy dependence of
 e^+e^- pair production
probability by high-energy
gamma-quanta

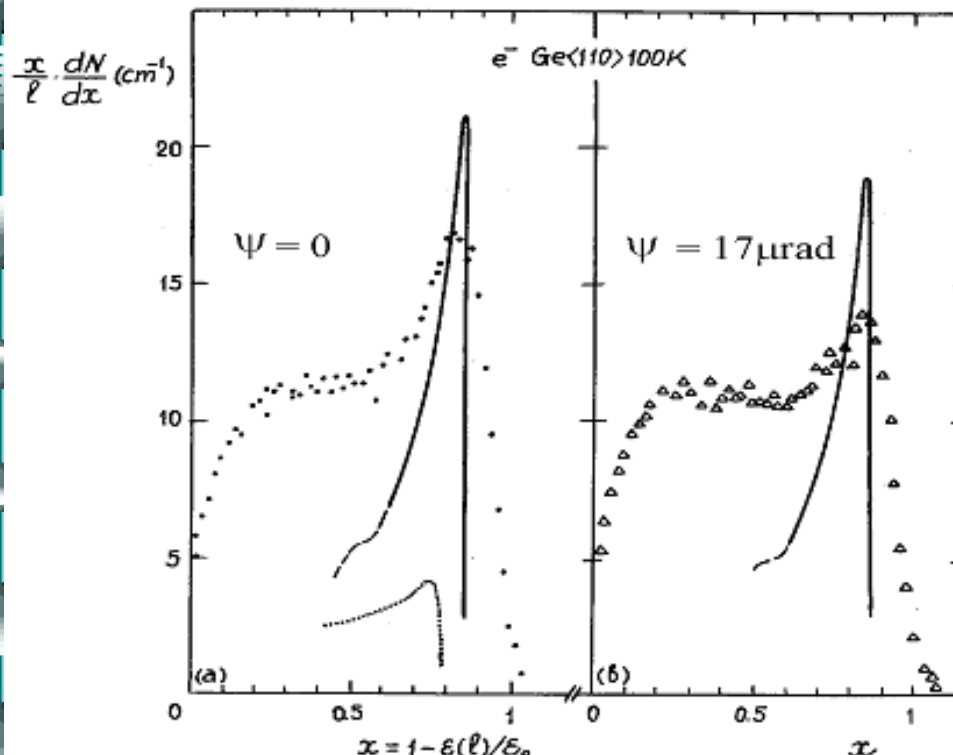
in the field of $<110>$ axes of a Ge
crystal at $T=100K$ expressed in
units of the Bethe – Heitler
probability.

Dots – **experimental data**. The
solid and dotted curves are
respectively calculated with and
without taking into account of the
energy dependence of the
probability of incoherent PP.



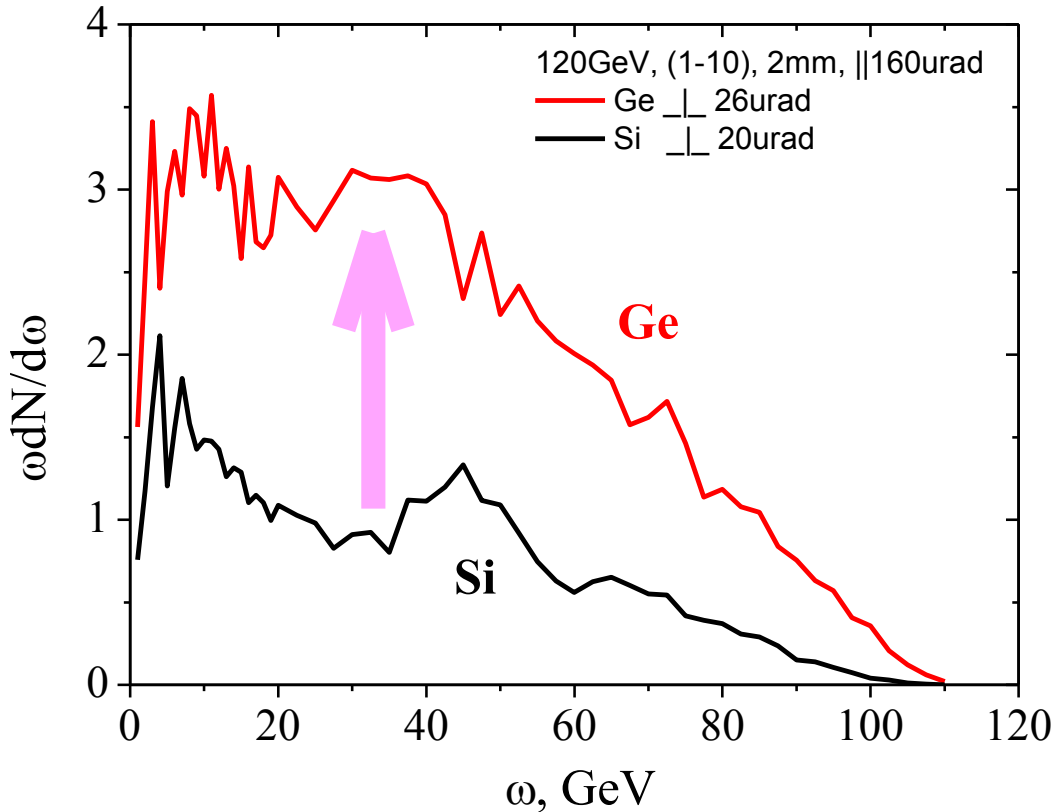
Electron radiative cooling in crystals

Tikhomirov V.V. Phys. Lett. A. 125(1987) 411; NIM B36(1989)282.



Electron radiative loss spectrum expressed in units of electron initial energy **150 GeV** at the angle of incidence $\Psi = 0$ and $17 \mu\text{rad}$ on the Ge crystal plane $\langle 110 \rangle$ cooled to 100K . Dotted curve is calculated without taking into account the radiation cooling.

Photon emission under the MVROC conditions



In Germanium ***two times more*** photons are radiated

Both strong crystal fields and high γ - quantum energies allow to reach the CRITICAL FIELD

$$E_0 = \frac{m^2 c^3}{e \hbar} = 1.32 \cdot 10^{16} \frac{\text{V}}{\text{cm}}$$

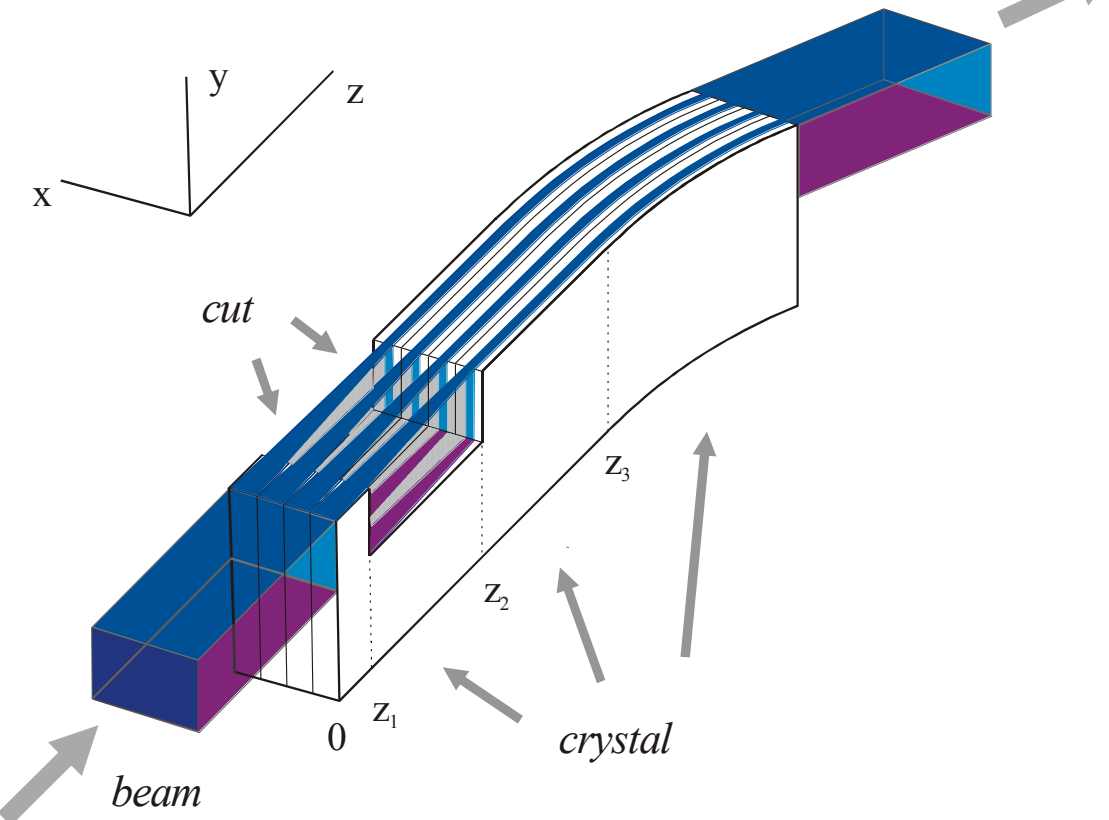
Table: Maximum electric fields and critical energies for some crystals

Crystal	(plane) or <Axis>	E_{\max} GV/cm	$\omega_{th} = \frac{2E_0}{E_{\max}} mc^2$ *
Diamond	(110)	7.7	1.78
	<110>	75	0.20
Si	(110)	5.7	2.39 (1.7)
	<110>	4.6	0.29
Ge	(110)	9.9	1.37 (0.9)
	<110>	78	0.174(0.11)
W	(110)	43	0.316
	<111>	500	0.027

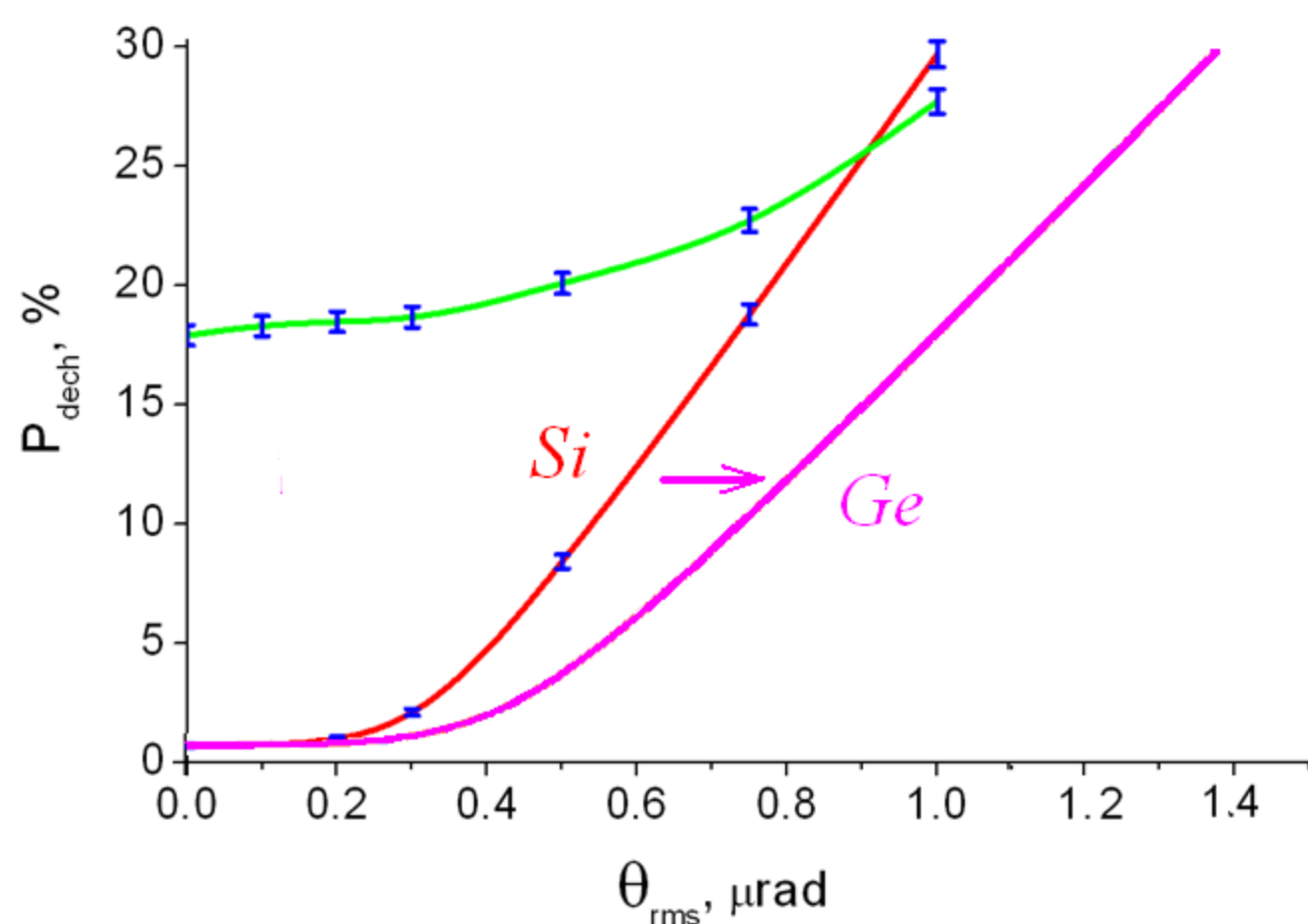
* Electric field reaches E_0 in ref. frame of $e^+ e^-$ pair produced at $\omega = \omega_{th}$

The capture probability **increase** by crystal cut

V.V.Tikhomirov, JINST, 2(2007)P08006

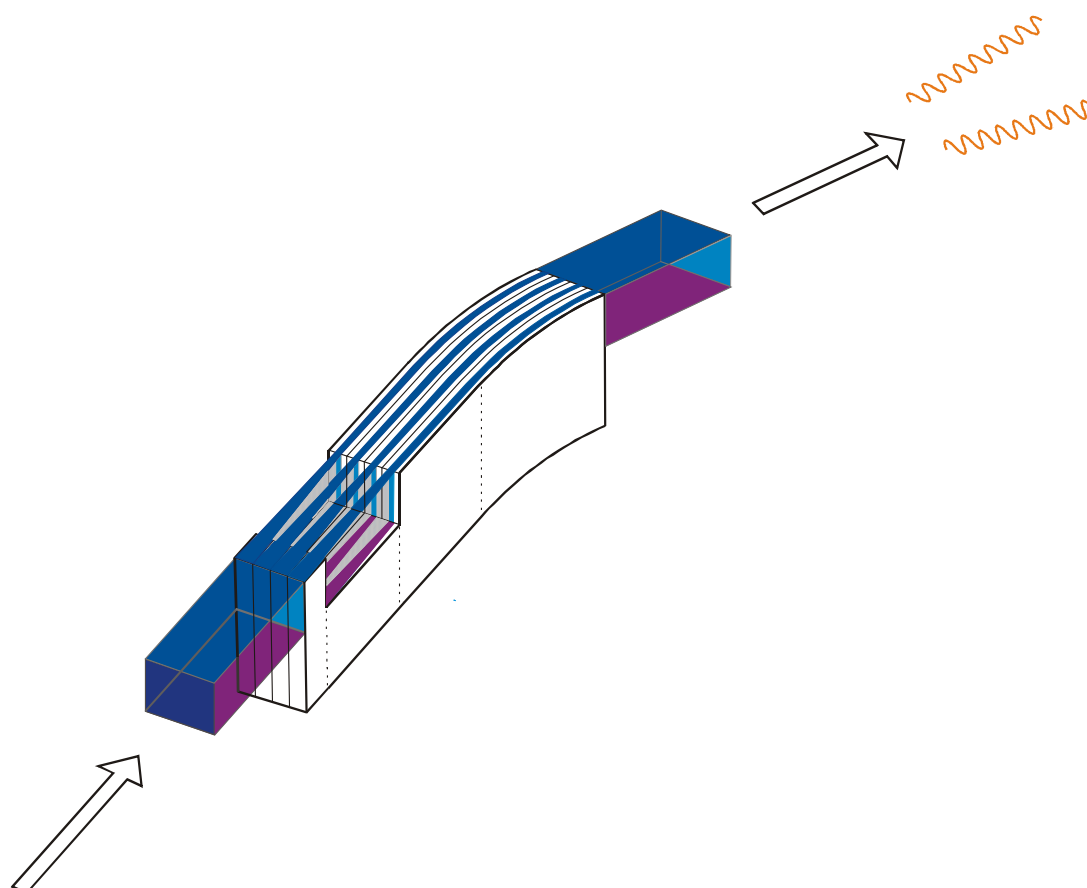


Improvement of the cut action in Ge



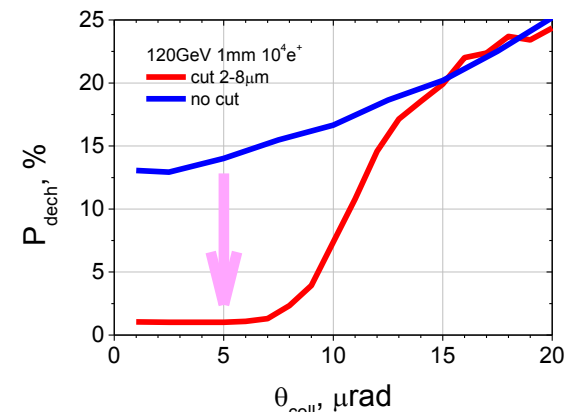
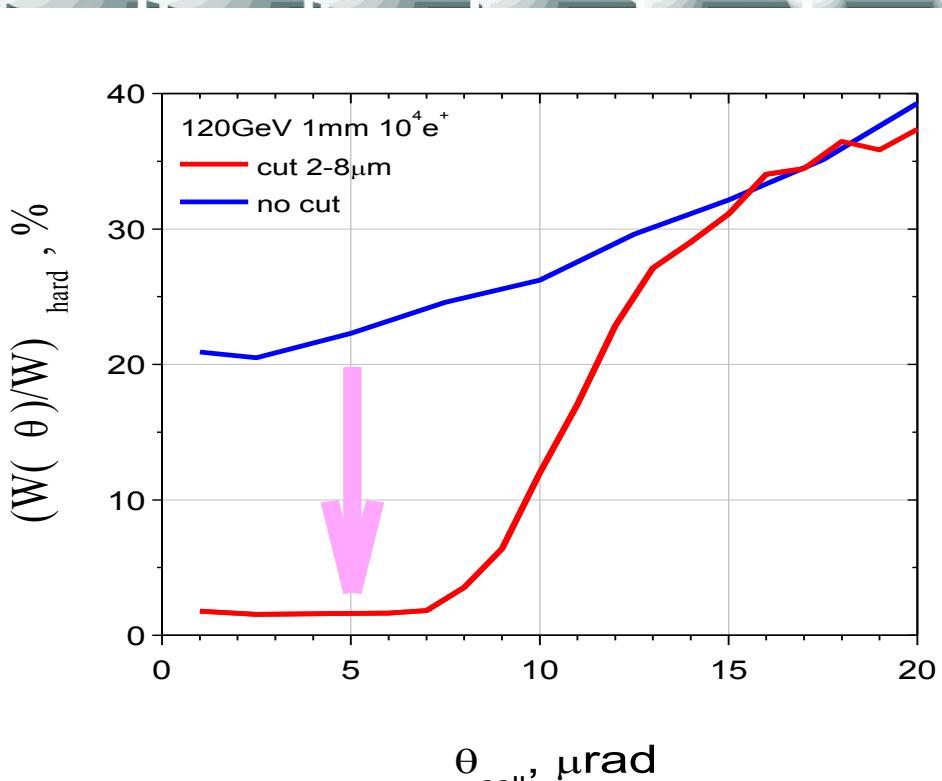
Ge widens the cut acceptance by 40%

Incoherent radiation **suppression** by crystal cut



Cut influence on the hard (Bethe-Heitler) part of radiation spectrum

$$\Delta W_{BH}(\theta) \equiv \int_{\omega_{\min}}^{\omega_{\max} = \varepsilon - mc^2} \frac{dW_{BH}(\theta)}{d\omega} d\omega$$



What is suggested to observe in the near future

**Circularly polarized Coherent Bremsstrahlung
and Pair Production.**

Allow to generate:

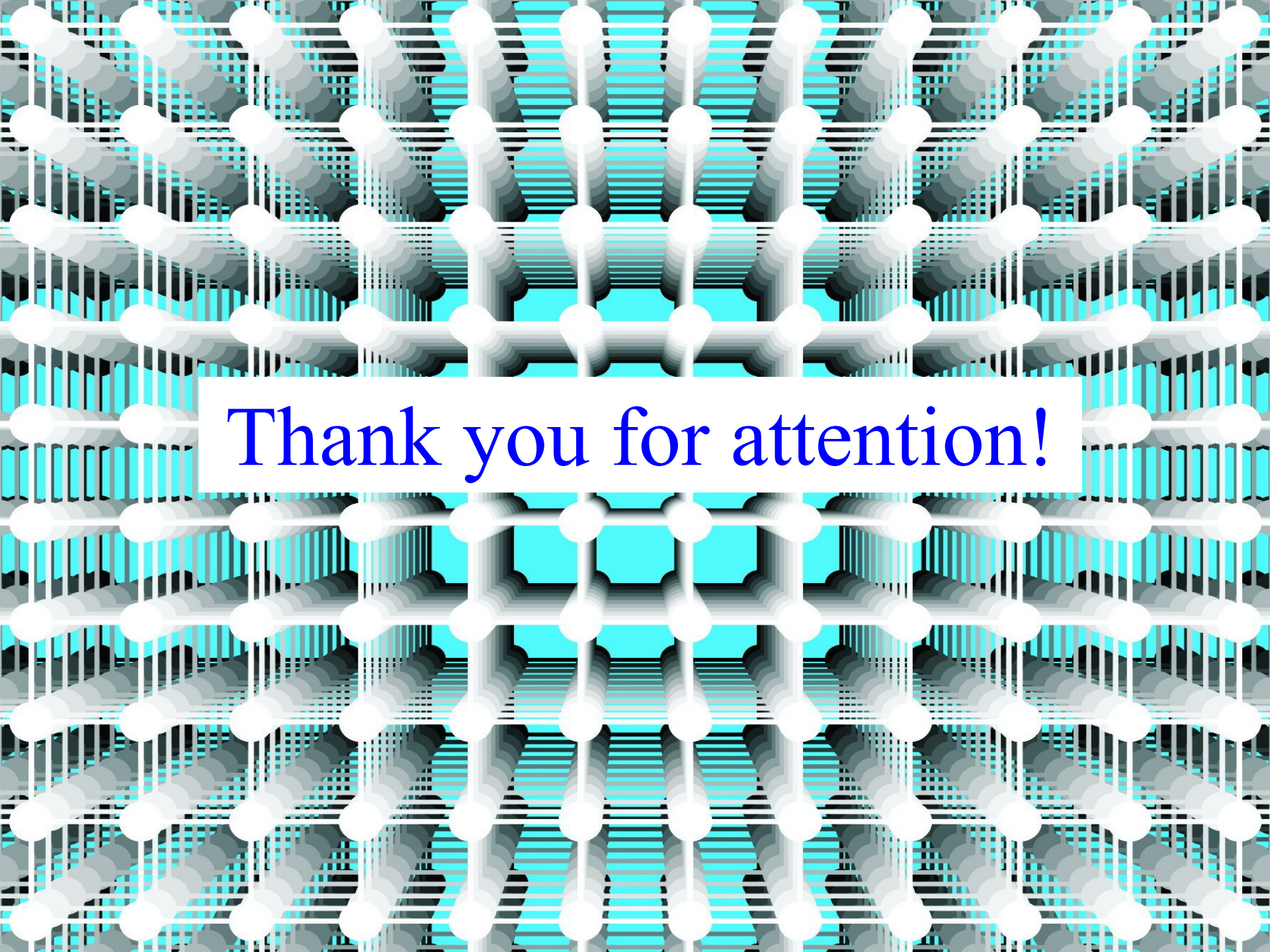
circularly polarized gamma-quanta,
longitudinally polarized positrons,
longitudinally polarized *electrons*.

Allow to measure:

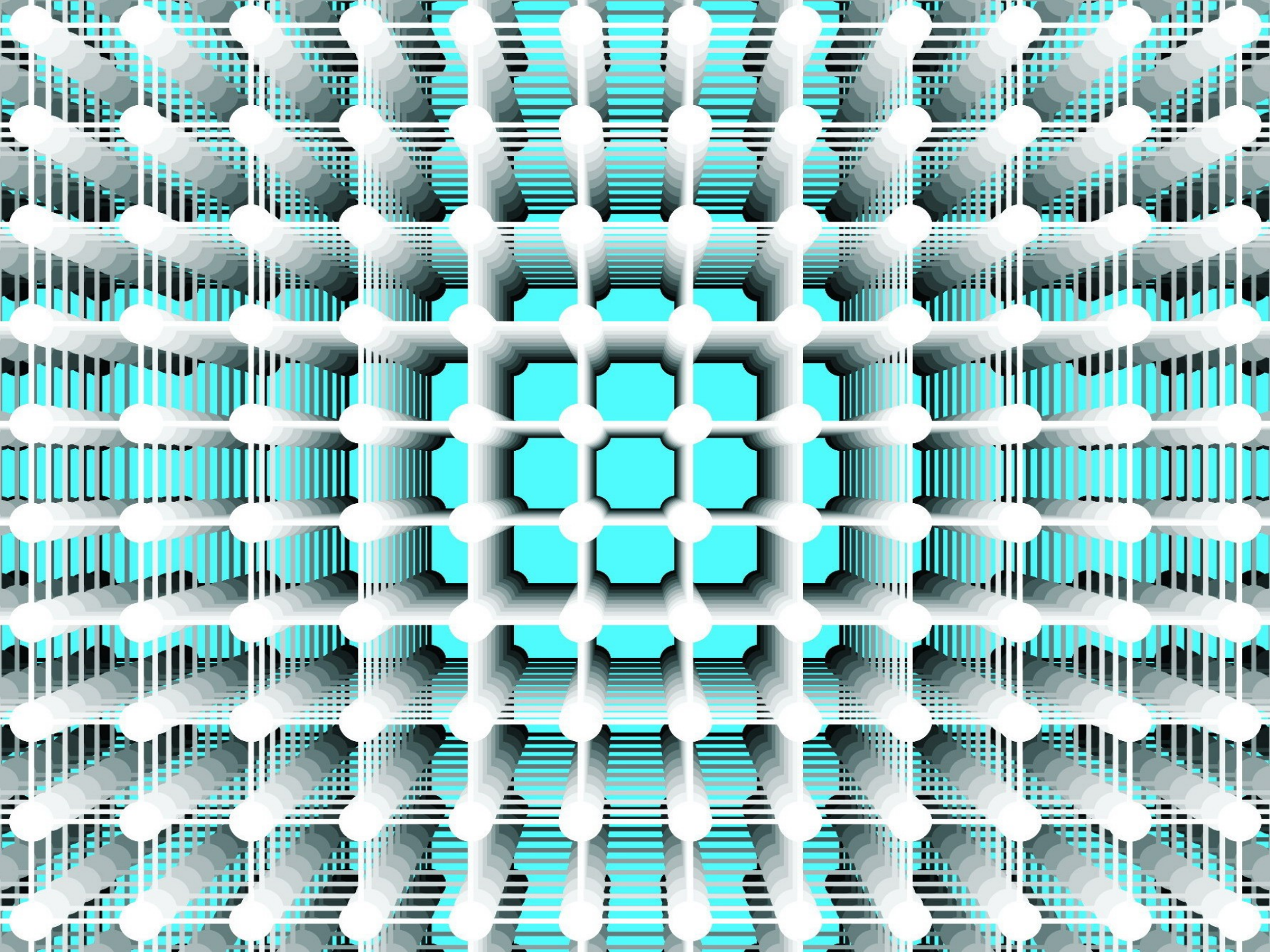
gamma circular polarization,
longitudinal positron polarization.

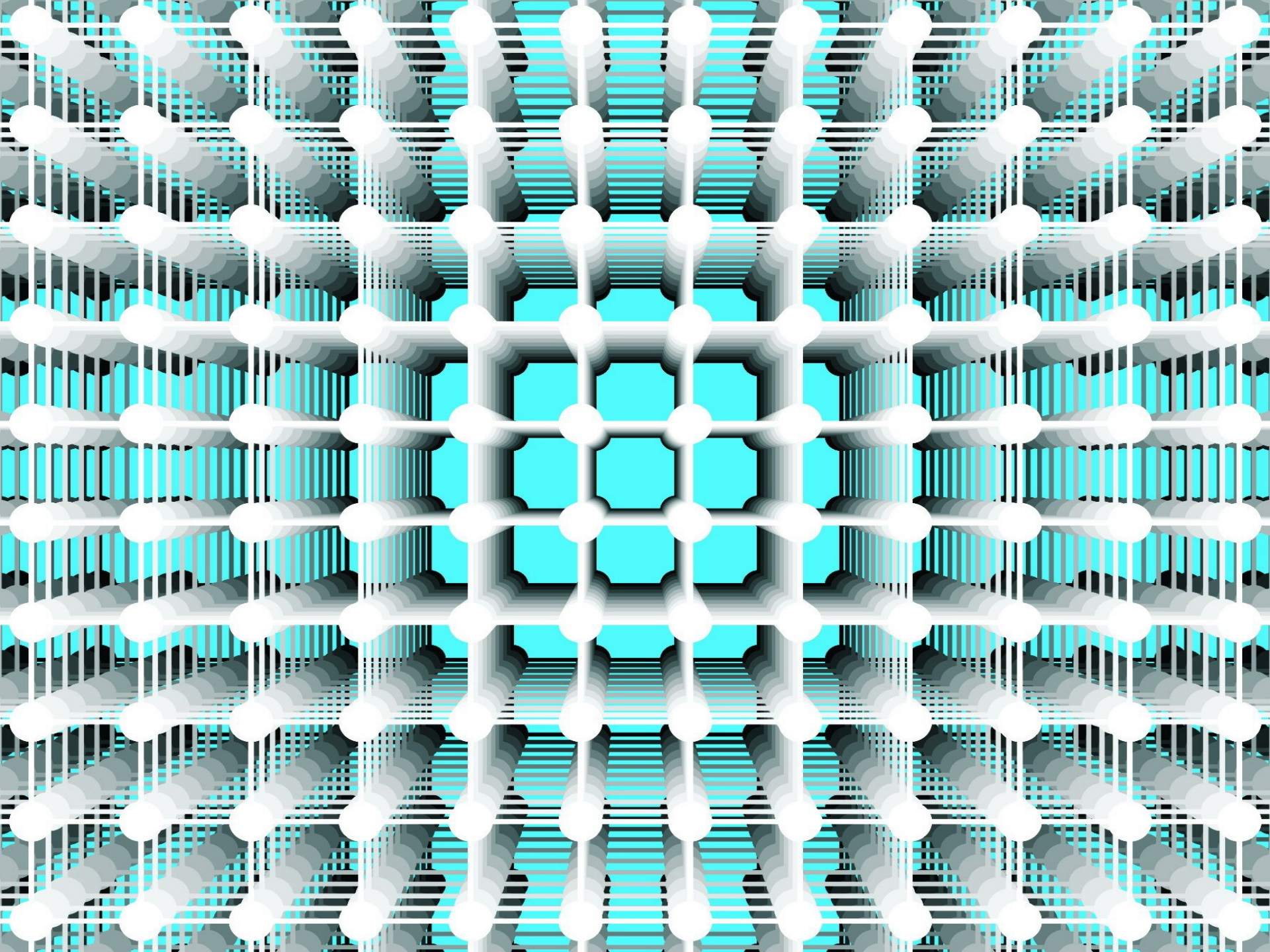
Radiation in the MVROC conditions.

Incoherent radiation suppression by crystal cut.



Thank you for attention!





Both strong crystal fields and high γ - quantum energies allow to reach the CRITICAL FIELD

$$E_0 = \frac{m^2 c^3}{e \hbar} = 1.32 \cdot 10^{16} \frac{\text{V}}{\text{cm}}$$

Table: Maximum electric fields and critical energies for some crystals

Crystal	(plane) or <Axis>	E_{\max} GV/cm	$\omega_{th} = \frac{2E_0}{E_{\max}} mc^2$ *
Diamond	(110)	7.7	1.78
	<110>	75	0.20
Si	(110)	5.7	2.39 (1.7)
	<110>	4.6	0.29
Ge	(110)	9.9	1.37 (0.9)
	<110>	78	0.174(0.11)
W	(110)	43	0.316
	<111>	500	0.027

* Electric field reaches E_0 in ref. frame of $e^+ e^-$ pair produced at $\omega = \omega_{th}$

Outline

- Coherent bremmstrahlung and its linear polarization
- String-of-strings crystal orientation
- Polarization of crystal field harmonics
- Circular polarization of radiation of positrons channeled in bent crystals with string-of-strings orientation
- Polarization asymmetry of channeled positron production
- Other manifestations of circular polarization of the crystal field harmonic
- Conclusions

What is suggested to observe:

e^+e^- pair production in semi-uniform field crystal field
Electron radiative cooling

Strong Field QED effects observable only at the *LHC* energy:

Synchrotron-like (**uniform field**) **dichroism**
and birefringence in very hard γ -region

Spin effects in bent crystal:

Radiative **self-polarization** in bent crystals
Production of transversely **polarized e^\pm**
by γ -quanta in bent crystals

Positron *magnetic moment modification*